This paper was published in Relibility Engineering & System Safety. Please cite it as:
Celano F, Dolšek M. Fatality risk estimation for industrialized urban areas considering multi-hazard domino effects triggered by earthquakes, Relibility Engineering & System Safety, 2021, 206, 107287, https://doi.org/10.1016/j.ress.2020.107287.

Fatality risk estimation for industrialized urban areas considering multi-hazard domino effects triggered by earthquakes

Francesca Celano[1], Matjaž Dolšek[1]

[1]Faculty of Civil and Geodetic Engineering, University of Ljubljana, Jamova 2, SI1000, Ljubljana, Slovenia

Abstract

The rapid expansion of the built environment has resulted in the coexistence of industrial facilities and urban centres. Following recent major earthquakes throughout the world, it has become clear that multi-hazard domino effects can significantly increase the risk of fatalities, environmental problems and losses. This complex phenomenon is not yet well understood. In this paper, the problem is treated by decomposing it into several subproblems which are described by simplified probabilistic models. These models are then coupled with the Monte Carlo method to estimate the annual probability of fatality for an individual who is continuously standing in a location of interest and to estimate fatality risk maps for an area of interest. Emphasis is placed on considering multi-hazard domino effects, which can be triggered within an industrial area due to the damage caused by earthquakes. Thus it is considered that fatalities can be caused: a) as a direct consequence of seismic damage to a unit b) as a direct physical and/or chemical consequence due to the loss of containment of hazardous material, and c) as a consequence of domino triggered by physical and chemical events such as fire, explosion, and toxic dispersion. The capabilities of the proposed methodology are demonstrated by calculating fatality risk maps for a hypothetical industrialized urban area. It is shown that disregarding multi-hazard domino effects in the estimation of fatality risk could lead to significant underestimation of the fatality risk in an industrialized urban area. Thus, it is necessary to account for multi-hazard domino effects. However, different teams of engineers can enhance the models for the probability of fatality due to various phenomena, which will improve the accuracy of the proposed methodology.

Keywords: multi-hazard risk assessment; domino effects; fatality risk; industrialized urban area; seismic risk

1. Introduction

Industrial facilities are essential components of the built environment. They provide vital services for the everyday functioning of a community, and often coexist with urban centres due to the rapid expansion of the built environment. This situation increases the exposure of urban centres to Natech events. It can happen that during major natural events such as earthquakes, a hazardous material is released in an industrial facility, which can result in catastrophes for the surrounding communities [1]. For instance, a seismic event can cause damage to a tank or a vessel. As a result, the hazardous material stored inside the tank may leak, which may trigger a fire, explosion, and/or some other adverse consequence. Such adverse events can then cause damage to other components of the facility as well as other residential buildings in the area, even if they have not been directly damaged by the earthquake, as was observed during the Fukushima earthquake in 2011 [2]. Additionally, the release of hazardous material can cause the dispersion of toxic gases into the environment and affect society, even far from industrial facilities. This propagation of damage is called the domino effect, which can be defined as an incident that starts in one unit of industrial facility and may affect nearby structures by thermal effects, a blast, or fragment impact, causing an increase in the severity of the consequences [3].

In order to understand and mitigate the potential consequences of the phenomena described above, it must be recognized that an industrialized urban area is a complex system, composed of industrial units (such as tanks and pipe racks) and residential buildings. Many studies have addressed the quantitative assessment of the performance of such complex systems by considering domino effects. Salzano and Cozzani [4] revised the available models for the analysis of domino accidents in industrial facilities triggered by explosions. In particular, they estimated the probability of damage to process equipment as a function of the intensity of the explosion and the distance from the explosion centre. Cozzani et al. [5] developed an algorithm for the quantitative assessment of the domino effect, based on a methodology which allowed the identification of domino scenarios and the assessment of consequences. Later on, a performance assessment methodology was

introduced for gas distribution networks, through the definition of a performance index which could be used for any type of natural or artificial hazard that might lead to a disruption of the system [6]. Several authors have investigated possibilities for improving the performance of industrial facilities. For example, Ahumada et al. [7] developed a methodology to optimize facility layout by evaluating the minimum distances of separation between process units in order to prevent the propagation of damage after the release of hazardous material. Due to the complexity of the problem, domino effects are often simulated using the Monte Carlo (MC) method. Abdolhamidzadeh et al. [8] proposed an algorithm which generates hypothetical experiments in order to simulate the behaviour of a complex system which might experience a domino effect, and then calculated the probability of failure for each unit of the system. The MC method was also used by Ramírez-Marengo et al. [9] to investigate the risk of vapour cloud explosions after a loss of hazardous material containment from different types of equipment (e.g. pipes, vessel, valves). Furthermore, Alessandri et al. [10] used MC simulations for the analysis of domino effects. They developed software which could be used to implement MC simulations in the case of tank farms.

While the contributions mentioned above and many other studies (e.g.[11,12]) offer comprehensive methodologies for the assessment of consequences by considering domino effects, it is still a challenge to conduct risk analysis by considering domino effects in the case of Natech events triggered by earthquakes. Therefore, a methodology for the calculation of fatality risk for industrialized urban areas considering multi-hazard domino effects triggered by earthquakes is proposed in this paper. However, the fatality risk is often considered as the main performance objective for the design of structures. For example, Tsang and Wenzel (2016) [13] performed pioneering research by using casualty data collected from past earthquakes around the worlds to develop the target collapse risk limits for structural design. In their approach, they considered the risk of fatality due to the collapse of buildings. Later on, Lazar Sinković and Dolšek (2020) [14] demonstrated a fatality risk-based decision model for the performance assessment of buildings with an emphasis on the consequences of the collapse of the building. Determining a tolerated level of risk, however, is a challenging task. Tsang et al. (2018) [15] developed a scenario-based methodology to calculate societal risk functions. In their approach, the number of fatalities is computed for each earthquake scenario and is plotted versus the rate of exceedance of the earthquake in order to obtain an F-N curve. From an F-N curve, it is possible to calculate the expected number of fatalities in the region, which was demonstrated by Tsang et al. (2020) [16] aimed at deriving societal risk functions at the national level.

In this study, the fatality risk is measured as individual risk (IR), which is defined as the annual probability of fatality for an individual who is continuously standing for one year at a point in the area of interest [17,18]. In the first part of the paper, the computation of IR in industrialized urban areas is described. The methodology requires the identification of units (e.g. tanks, pipe racks, offices, storage warehouses, residential buildings etc.), the definition of seismic fragility functions, and information about the seismicity of the location. Moreover, models for estimating the probability of fatality, the probability of Loss Of Containment (LOC), and models for simulating physical-chemical consequences due to LOC, are also needed. These models are then coupled by the MC method, which allows the simulation of thousands of possible scenarios of damage propagation. In the second part of the paper, the methodology is demonstrated by calculating the fatality risk maps for a simple industrialized urban area. Emphasis is put on the difference in the results with and without consideration for the domino effects. Finally, possibilities for decision-making using the information from fatality risk maps is briefly discussed, with an emphasis on safety issues in industrialized urban areas.

2. Probabilistic framework for the estimation of earthquake fatality risk

In order to compute the IR, the industrialized urban area of interest is discretised into a grid of points, each of which is analysed separately. This is in accordance with the guidelines provided by the Purple Book [17], entitled "Guideline for quantitative risk assessment" and prepared by The Netherlands Organization of Applied Scientific Research (TNO). In the process of evaluating IR, the points in the grid are termed *targets*, while the units are the *sources*.

This paper was published in Relibility Engineering & System Safety. Please cite it as:
Celano F, Dolšek M. Fatality risk estimation for industrialized urban areas considering multi-hazard domino effects triggered by earthquakes, Relibility Engineering & System Safety, 2021, 206, 107287, https://doi.org/10.1016/j.ress.2020.107287.

The probabilistic formulations in the following subsections provide the framework for calculating the IR at each target in the area of interest. In the first subsection, the conditional probability of fatality caused by earthquakes, the (mean) annual fatality rate, and the IR are introduced. The method for estimating the probability of fatality due to the damage state of each unit is described in the second subsection. This probability of fatality is calculated by the MC method, as presented in the third subsection. Finally, the entire methodology for calculating the IR and deriving the fatality risk maps is summarized in Subsection 2.4.

2.1 Annual rate of fatality and individual risk (IR)

In the proposed methodology, earthquakes (*Eqs*) are the events which can cause the fatality, either directly as a consequence of damage to the unit, or indirectly via domino effects. With reference to the grid of targets in Figure 1, a system composed of n_U units is considered. If an earthquake occurs, the *i-th* unit, U_i, may suffer damage $D(U_i)$ and cause the fatality of an individual located at the target with coordinates (x,y) (Figure 1).

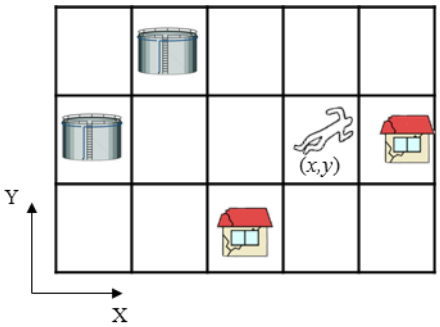

Figure 1. Discretization of the area of interest in a grid of targets, with the indication of the units and the target with coordinates (x,y)

The annual rate of fatality for an individual located at target (x,y), $\lambda(x,y)$, can be obtained by multiplying the rate of occurrence of earthquakes in a specific location, ν, by the probability of fatality due to earthquakes, $P[F(x,y)\,|\,Eqs]$:

$$\lambda(x,y) = \nu \cdot P[F(x,y)\,|\,Eqs] \tag{1}$$

By considering the total probability theorem, the $P[F(x,y)\,|\,Eqs]$ is decomposed into the conditional probability of fatality for a given intensity level of an earthquake, $P[F(x,y)\,|\,IM = im]$, and the probability of an earthquake of intensity level $IM = im$. The $P[F(x,y)\,|\,Eqs]$ can then be obtained by summing (integrating) the product of these quantities over the entire range of intensity levels. Thus Eq. (1) can be transformed to:

$$\lambda(x,y) = \int \nu \cdot P[F(x,y)\,|\,IM = im]\, f_{IM}(im)\, d\,im \tag{2}$$

where $f_{IM}(im)$ is the probability density function for the intensity measure. It can be shown [19] that the product $\nu \cdot f_{IM}(im) \cdot d\,im$ is the derivative of the hazard function λ_{IM}, which expresses the mean annual frequency of exceeding a given intensity measure. Therefore, Eq. (2) can be rewritten as:

$$\lambda(x,y) = \int P[F(x,y)\,|\,IM = im] \left| d\,\lambda_{IM} \right| \tag{3}$$

The conditional probability of fatality $P[F(x,y)\,|\,IM = im]$ expresses the probability of fatality due to the damage to any of the n_U units in the system. This probability can be obtained as the probability of the union of all fatality events caused by the damage of each unit separately:

This paper was published in Relibility Engineering & System Safety. Please cite it as:
Celano F, Dolšek M. Fatality risk estimation for industrialized urban areas considering multi-hazard domino effects triggered by earthquakes, Relibility Engineering & System Safety, 2021, 206, 107287, https://doi.org/10.1016/j.ress.2020.107287.

$$P[F(x,y)\,|\,IM=im]=P\left[\bigcup_{i=1}^{n_U}F(x,y)\,|\,D(U_i),IM=im\right] \tag{4}$$

where $F(x,y)\,|\,D(U_i),IM=im$ is the fatality event due only to the damage of the *i-th* unit. It is important to note that the probability of the union is not the sum of the probabilities of single events because the fatality events are not mutually exclusive. Indeed, it may happen that two units are damaged by a seismic event, and then a third unit is damaged because of the domino effect, and all three damaged units can cause the fatality of an individual, directly or indirectly, at almost the same time. In such a case, the individual would die due to the first fatality event. Therefore, the probability of dying from the other fatality events shall be disregarded in the evaluation of the IR. This can be achieved by solving the probability of the union of fatality events in Eq.(4). For example, if the number of units that can cause a fatality is equal to two, n_U=2, the probability that an earthquake characterized by an intensity measure $IM=im$ causes a fatality at target (*x*,*y*) (i.e. Eq.(4)) is obtained as follows:

$$\begin{aligned}P[F(x,y)\,|\,IM=im]&=P[F(x,y)\,|\,D(U_1),IM=im]+P[F(x,y)\,|\,D(U_2),IM=im]\\&-P[(F(x,y)\,|\,D(U_1),IM=im)\cap(F(x,y)\,|\,D(U_2),IM=im)]\end{aligned} \tag{5}$$

In the case if n_U=3, Eq. (4) is expressed as follows:

$$\begin{aligned}&P[F(x,y)\,|\,IM=im]=\\&\quad=P[F(x,y)\,|\,D(U_1),IM=im]+P[F(x,y)\,|\,D(U_2),IM=im]+P[F(x,y)\,|\,D(U_3),IM=im]\\&\quad-P[(F(x,y)\,|\,D(U_1),IM=im)\cap(F(x,y)\,|\,D(U_2),IM=im)]\\&\quad-P[(F(x,y)\,|\,D(U_1),IM=im)\cap(F(x,y)\,|\,D(U_3),IM=im)]\\&\quad-P[(F(x,y)\,|\,D(U_2),IM=im)\cap(F(x,y)\,|\,D(U_3),IM=im)]\\&\quad+P[(F(x,y)\,|\,D(U_1),IM=im)\cap(F(x,y)\,|\,D(U_2),IM=im)\cap(F(x,y)\,|\,D(U_3),IM=im)]\end{aligned} \tag{6}$$

The probability of the intersection of events (e.g. $P[(F(x,y)\,|\,D(U_1),IM=im)\cap(F(x,y)\,|\,D(U_2),IM=im)]$) accounts for the case in which two or more units, which are damaged by an earthquake with $IM=im$, cause the fatality of an individual located at target (*x*,*y*) at almost the same time. If these events can be considered independent, then the probability of the intersection can be obtained simply by multiplying the probabilities of the single events, as follows:

$$\begin{aligned}&P[(F(x,y)\,|\,D(U_i),IM=im)\cap(F(x,y)\,|\,D(U_j),IM=im)]=\\&\quad=P[(F(x,y)\,|\,D(U_i),IM=im)]\cdot P[(F(x,y)\,|\,D(U_j),IM=im)]\end{aligned} \tag{6}$$

However, such events may not be independent. For example, if the two units are similar, there is a certain probability that the two units would suffer the same damage because of an earthquake. In the hypothetical case when two identical units are hit by the same ground motions, the damage to these units would be identical, and the probability of fatality due to damage of the *i-th* unit is equal to the probability of fatality due to damage of the *j-th* unit. In this case, the probability of the intersection is equal to the probability of single events:

$$\begin{aligned}&P[(F(x,y)\,|\,D(U_i),IM=im)\cap(F(x,y)\,|\,D(U_j),IM=im)]=\\&\quad=P[(F(x,y)\,|\,D(U_i),IM=im)]=P[(F(x,y)\,|\,D(U_j),IM=im)]\end{aligned} \tag{7}$$

This paper was published in Relibility Engineering & System Safety. Please cite it as:
Celano F, Dolšek M. Fatality risk estimation for industrialized urban areas considering multi-hazard domino effects triggered by earthquakes, Relibility Engineering & System Safety, 2021, 206, 107287, https://doi.org/10.1016/j.ress.2020.107287.

In realistic cases, even if the two units are nominally identical, their performance is not identical due to aleatoric uncertainty. Thus, the probability of the intersection of fatality events varies between that defined by Eq. (7) and that defined by Eq.(8). It should be noted that a realistic estimation of the probability of the intersection would require a seismic response history analyses of the entire complex system, as well as a physics-based simulation of the domino effects (e.g. vapour cloud explosions, dispersion of toxic gas). Such an approach is too complicated for practical or even for scientific applications. In this study, it is thus assumed that the probability of the intersection of fatality events is calculated by considering these events to be independent (Eq. (7)). This assumption provides conservative results.

The remaining challenge is to assess the probability of fatality due to the damage of a single unit, $P[(F(x,y)\,|\,D(U_i), IM = im)]$. However, it must be realized that the damage of a unit can vary significantly. Therefore, it is necessary to account for the severity of the damage, which is usually modelled by a set of damage states. Defining $n_{DS,i}$ as the number of damage states considered for the *i-th* unit, the probability $P[(F(x,y)\,|\,D(U_i), IM = im)]$ can then be calculated by utilizing the total probability theorem:

$$P[(F(x,y)\,|\,D(U_i), IM = im)] = \sum_{d=1}^{n_{DS,i}} P[F(x,y)\,|\,D(U_i) = DS_d] \cdot P[D(U_i) = DS_d\,|\,IM = im] \tag{8}$$

where $D(U_i) = DS_d$ represents the *d-th* discrete damage state of the *i-th* unit. The probability that the *d-th* discrete damage state of the *i-th* unit is observed for an earthquake with intensity $IM = im$, $P[D(U_i) = DS_d\,|\,IM = im]$, can be derived from seismic fragility functions:

$$P[D(U_i) = DS_d\,|\,IM = im] = P[D(U_i) \geq DS_d\,|\,IM = im] - P[D(U_i) \geq DS_{d+1}\,|\,IM = im] \tag{9}$$

where $P[D(U_i) = DS_{d+1}\,|\,IM = im]$ and $P[D(U_i) = DS_d\,|\,IM = im]$ are the seismic fragility functions evaluated at seismic intensity $IM = im$, as presented in Figure 2. The probabilities $P[D(U_i) = DS_d\,|\,IM = im]$ shown in Figure 2 are based on four different damage states, for a generic level of intensity measure $IM = im$. Many different methods for the evaluation of the seismic fragility functions exist (e.g. [20]). For simplicity, these methods are not discussed in detail. However, examples of seismic fragility functions for different kind of structures may be found elsewhere (e.g. [21,22]).

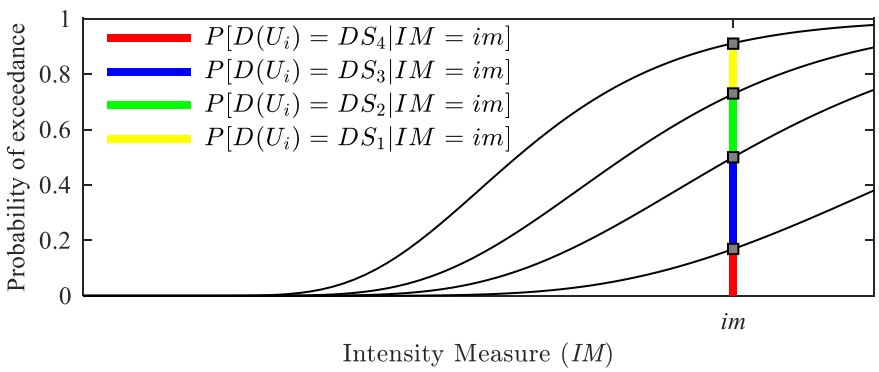

Figure 2. Schematic representation of the evaluation of $P[D(U_i) = DS_d\,|\,IM = im]$ *from the seismic fragility functions*

By substituting Eq. (9) into Eq. (4), the annual rate λ of a fatality for an individual located at target (x,y) (Eq. (3)) can be expressed in the following form:

$$\lambda(x,y) = \int \bigcup_{i=1}^{n_U} \left(\sum_{d=1}^{n_{DS,i}} (P[F(x,y)\,|\,D(U_i) = DS_d] \cdot P[D(U_i) = DS_d\,|\,IM = im]) \right) \cdot \left| d\lambda_{IM} \right| \tag{10}$$

This paper was published in Relibility Engineering & System Safety. Please cite it as:
Celano F, Dolšek M. Fatality risk estimation for industrialized urban areas considering multi-hazard domino effects triggered by earthquakes, Relibility Engineering & System Safety, 2021, 206, 107287, https://doi.org/10.1016/j.ress.2020.107287.

The remaining challenge for solving Eq. (11) is to calculate $P[F(x,y)\,|\,D(U_i)=DS_d]$, which will be described in Subsections 2.2 and 2.3.

If the fatality events can be assumed to be independent of time, the probability of fatality in the reference period Δt, can be modelled as a homogenous Poisson process in which the time between two successive deadly events follows an exponential distribution. Therefore, for a period Δt during which the rate of fatality $\lambda(x,y)$ can be considered constant, the probability $p(x,y)$ of fatality at target (x,y) can be computed as:

$$p(x,y)=1-e^{-\lambda(x,y)\cdot\Delta t} \tag{11}$$

Finally, the IR is calculated from Eq. (12) as the annual ($\Delta t=1$ year) probability of fatality for an individual located at target (x,y):

$$IR(x,y)=1-e^{-\lambda(x,y)}\approx\lambda(x,y) \tag{12}$$

The IR is practically equal to the annual fatality rate (Eq. (13)) because the fatality rate is usually a low number.

2.2 Model of fatality due to the damage state of a unit in a given area

The calculation of the probability of fatality due to the *d-th* discrete damage state of the *i-th* unit, $P[F(x,y)\,|\,D(U_i)=DS_d]$, is a much more elementary task than calculating the probability of fatality due to earthquakes, $P[F(x,y)\,|\,Eqs]$. However, it is still quite complicated to calculate $P[F(x,y)\,|\,D(U_i)=DS_d]$, because a fatality can be observed as a direct or even indirect consequence of damage to the *i-th* unit. If the unit is damaged, an individual at the target may die because of the direct impact of falling debris after the seismic damage. If the individual survives such an adverse event, he may still die because of chemical consequences due to the leakage of hazardous material. Furthermore, the damaged unit may trigger a domino effect, which may also cause a fatality. Therefore, it is necessary to establish fatality models which provide for all possible situations that can result in a fatality. In the framework of this study, the fatality model accounts for the three cases described as follows.

Fatality case a: Fatality as a direct consequence of seismic damage to a unit
In this case, the fatality is caused by the impact of debris that fall from the unit and hit the individual located at the target.

Fatality case b: Fatality as a direct consequence of LOC of a unit
In such a situation, the fatality is caused by the consequences of a loss of containment (LOC). There are many different kinds of mutually exclusive LOC states (indicated as LOC_1, LOC_2, and so go on), such as "instantaneous release", or "continuous release " [17]. The LOC states are caused by the seismic damage of a unit, and may trigger the following physical-chemical phenomena, which can consequently cause a fatality [23,24]:

- Toxic Dispersion (TD), which may cause fatality by the inhalation of the released toxic material;
- Pool Fire (PF), as a result of the ignition of released fuel, which may cause fatality because of heat radiation;
- Flash Fire (FF), i.e. the late ignition of dispersed vapour at a concentration within the flammability range of the fuel, which may cause fatality because of heat radiation;

This paper was published in Relibility Engineering & System Safety. Please cite it as:
Celano F, Dolšek M. Fatality risk estimation for industrialized urban areas considering multi-hazard domino effects triggered by earthquakes, Relibility Engineering & System Safety, 2021, 206, 107287, https://doi.org/10.1016/j.ress.2020.107287.

- Vapour Cloud Explosion (VCE), which can occur when a large quantity of flammable gas or vapour is accidentally released into the atmosphere and forms a vapour cloud with delayed ignition. In this case, the released energy and overpressure may cause fatality;
- Fireball (FB), caused by the slow and laminar combustion of a flammable cloud, which can cause fatality because of heat radiation.

Fatality case c: Fatality as a result of domino effects

Under some circumstances, it is considered that the LOC event triggers domino effects in the industrial facility or in the surrounding area. This means that damage to the *i-th* unit, caused by an earthquake, can indirectly cause damage to the *j-th* unit. As a consequence, the fatality event at target (x, y) can occur due to the debris of the *j-th* unit, as in *fatality case a*, or because of the consequences of LOC events of the *j-th* unit, as in *fatality case b*. Moreover, if the individual at target (x, y) still survives, a second-level of domino may be triggered, which may again cause fatality. This means that, in general, the model must show that damage to the *i-th* unit can cause a series of damage to other units in the area, and fatality at target (x, y) is then the consequence of *fatality case a* or *fatality case b* due to damage to other units.

The three fatality cases, which contribute to the probability of fatality at the target, can be visualised by the event tree in Figure 3. It should be noted that the branches of the event tree which follow LOC_2 and LOC_3 are not shown in the figure for the sake of simplicity, but these event trees have the same branches as those following LOC_1. The same simplification is considered in the non-representation of the event tree following VCE, FF, and FB. In those cases, the tree branches are the same as those following PF.

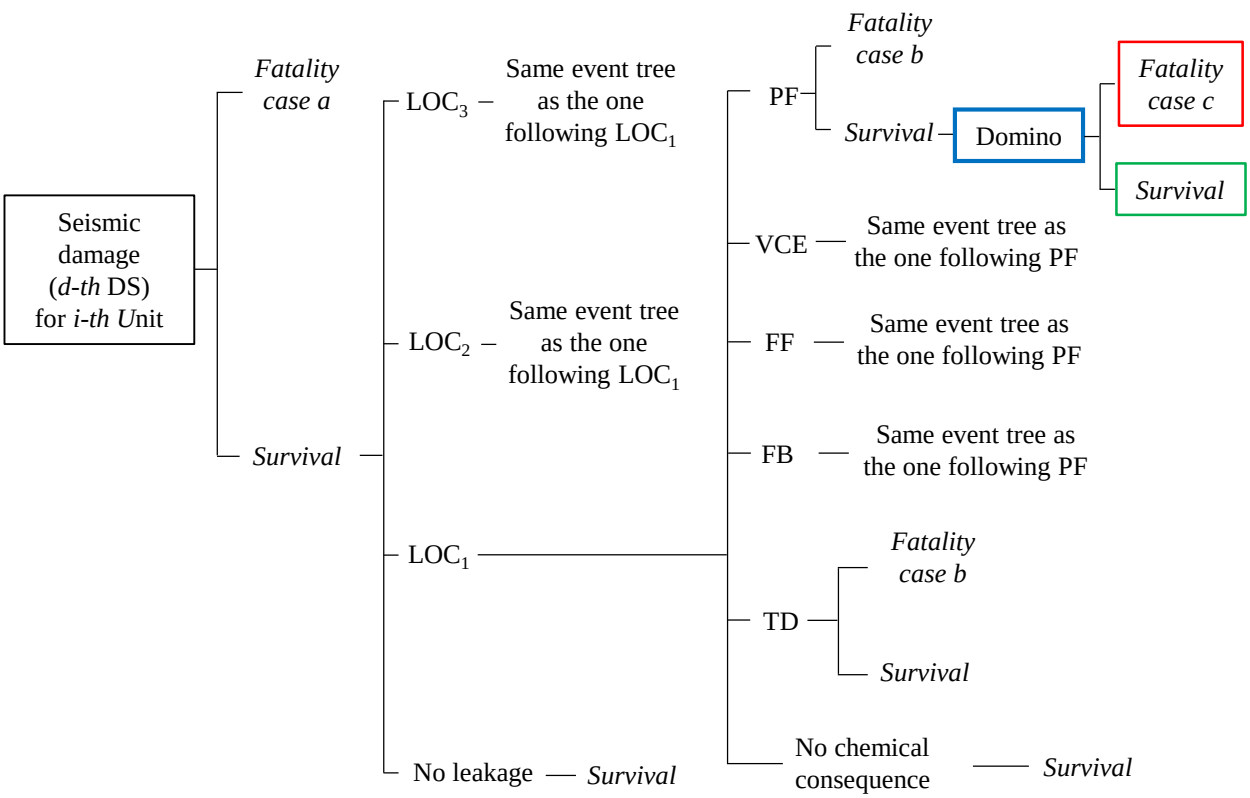

Figure 3. Event tree of events which can result in the fatality or in the survival of an individual continuously standing at the target. The event tree is only partly branched

The event tree (Figure 3) starts with the initiating event "*Seismic damage (d-th Damage State) for i-th Unit*", which triggers other possible events. Many different chains of events are possible by following different

This paper was published in Relibility Engineering & System Safety. Please cite it as:
Celano F, Dolšek M. Fatality risk estimation for industrialized urban areas considering multi-hazard domino effects triggered by earthquakes, Relibility Engineering & System Safety, 2021, 206, 107287, https://doi.org/10.1016/j.ress.2020.107287.

branches of the tree. Each intermediate event has a probability of occurrence, which can be calculated using several models, as described in the following sections. The event "domino" as marked in blue (Figure 3) is, in general, a further chain of event trees. This is schematically presented by the event tree in Figure 4. Note that the event tree in Figure 4 can end up with a "*Survival*" (green boxes in Figure 4), or with a "*Fatality*" (red boxes in Figure 4). The event "*Survival*" in the green box in Figure 3 refers to any of the events "*Survival*" from Figure 4. In the same way, the event "*Fatality case c*" in the red box in Figure 3 refers to any of the events "*Fatality*" from Figure 4.

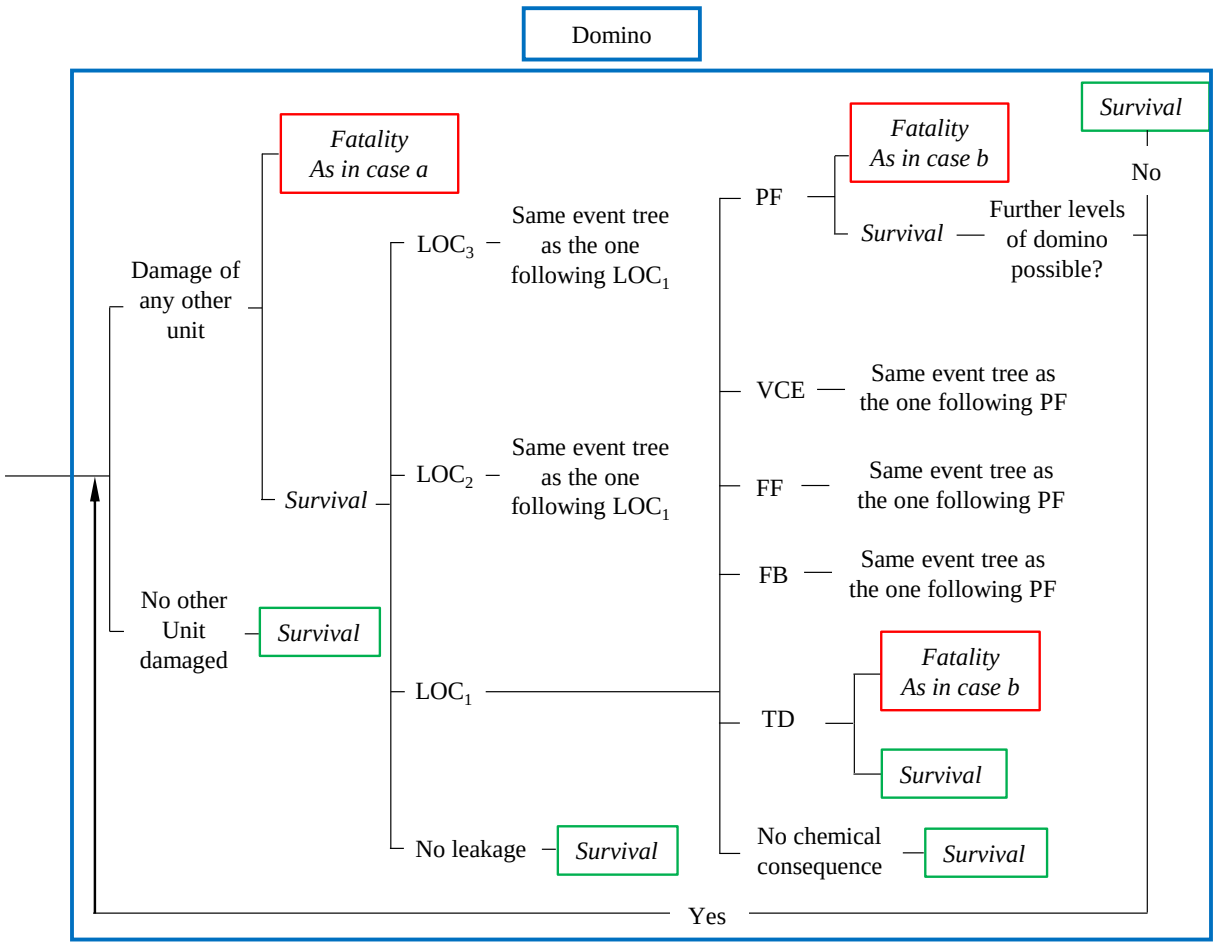

Figure 4. Event tree for fatality case c, which accounts for domino effects. The event tree is only partly branched

The triggering of a domino (starting node of the event tree in Figure 4) can cause damage to any other unit of the system. As a consequence of the damage of any other unit, a fatality may be caused by debris (as in *fatality case a*). Otherwise, a LOC state may be observed for the new damaged units, which may trigger physical-chemical consequences and cause fatality (as in *fatality case b*). If the individual still survives, the possibility of further levels of domino effects must be checked.

To clarify the interpretation of the event tree "domino", some examples of domino effects are presented in Figure 5. In the presented example, the system consists of four units, labelled A, B, C, and D, and fifteen targets, with an indication of a particular target T (Figure 5a). In the case of domino effects, several scenarios which cause fatality are possible. It may happen that unit A causes damage to unit B, which causes fatality in T (i.e. domino effects from A to B to T, Figure 5b), or that unit A causes damage to unit B, which in turn causes damage to unit D, which causes fatality in T (i.e. domino effects from A to B to D to T, Figure 5c), or many other scenarios. It is clear that the definition of all possible domino scenarios and the calculation of the

This paper was published in Relibility Engineering & System Safety. Please cite it as:
Celano F, Dolšek M. Fatality risk estimation for industrialized urban areas considering multi-hazard domino effects triggered by earthquakes, Relibility Engineering & System Safety, 2021, 206, 107287, https://doi.org/10.1016/j.ress.2020.107287.

probability of fatality may become quite complicated, especially if the system consists of many units. For this reason, scenarios for single or multi-level dominos and the corresponding probability of fatality are simulated by the MC method, as described in the following subsection.

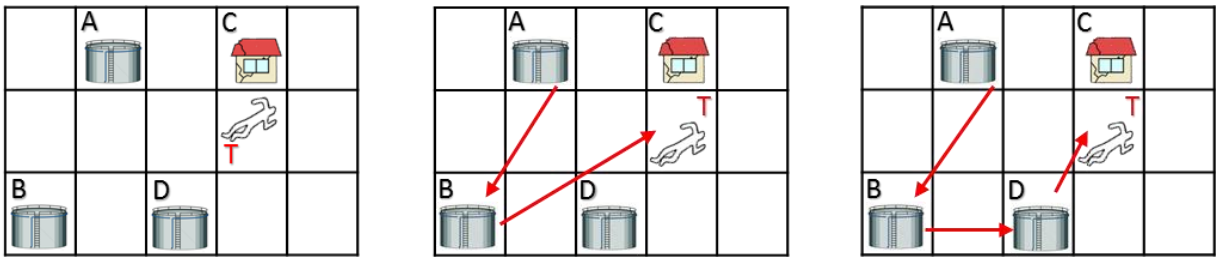

Figure 5. (a) Example of a grid of targets with an indication of the units and of the target T. Representation of possible domino scenarios: (b) domino effects from A to B to T; (c) domino effects from A to B to D to T

2.3 Estimation of the probability of fatality due to the damage state of a unit using the MC method

The MC method is used to calculate the probability of fatality at a target due to the *d-th* damage state of the *i-th* unit $P[F(x,y)\,|\,D(U_i)=DS_d]$. The procedure consists in sampling "*Fatality*" or "*Survival*" from the event trees in Figure 3 and Figure 4. Each event in the event trees has a probability of occurrence, which must be estimated in order to perform the MC simulations. Therefore, the following models of probability, which will be defined in Section 3, need to be developed:

- probability of fatality as a direct consequence of seismic damage to the unit (i.e. *fatality case a*): $P[F(a)]$
- probability of the occurrence of an LOC state: $P[LOC_k]$
- probability of the occurrence of physical-chemical phenomena as a consequence of LOC states: $P[PhCh|LOC_k]$
- probability of fatality caused by physical-chemical phenomena (i.e. *fatality case b*): $P[F(b)]$
- probability of a damage state in the other units, caused by physical-chemical phenomena $P[D(U)|PhCh]$

These models are the basis for sampling "*Fatality*" or "*Survival*", as described in the following. Firstly, every single simulation begins by generating a random number r_1 between 0 and 1. If r_1 is less than $P[F(a)]$, then a fatality has occurred, and the simulation is terminated. The outcome of the simulation is "*Fatality*" (Figure 6a). Otherwise, if r_1 is greater than $P[F(a)]$, the simulation continues on the following branch of the event tree. For example, if the *i-th* unit is not an industrial unit, there is no possibility for an LOC state. Therefore, the simulation follows the branch "*No leakage*". In this case, the outcome of the simulation is "*Survival*" (Figure 6b), and the simulation is terminated. On the contrary, if the *i-th* unit stores hazardous material, an LOC state has to be sampled. Each LOC state has a probability of occurrence $P[LOC_k]$. Because the LOC states are assumed to be mutually exclusive and collectively exhaustive, the sum of their probabilities of occurrence is equal to 1. Therefore the LOC state can be sampled by arranging the probabilities $P[LOC_k]$ between 0 and 1 (as schematically shown in Figure 7a) and by generating a random number r_{LOC} between 0 and 1 (i.e. red dot in Figure 7a). The physical-chemical phenomena are then sampled in the same manner (Figure 7b), by generating an additional random number r_{CONS} between 0 and 1.

This paper was published in Relibility Engineering & System Safety. Please cite it as:
Celano F, Dolšek M. Fatality risk estimation for industrialized urban areas considering multi-hazard domino effects triggered by earthquakes, Relibility Engineering & System Safety, 2021, 206, 107287, https://doi.org/10.1016/j.ress.2020.107287.

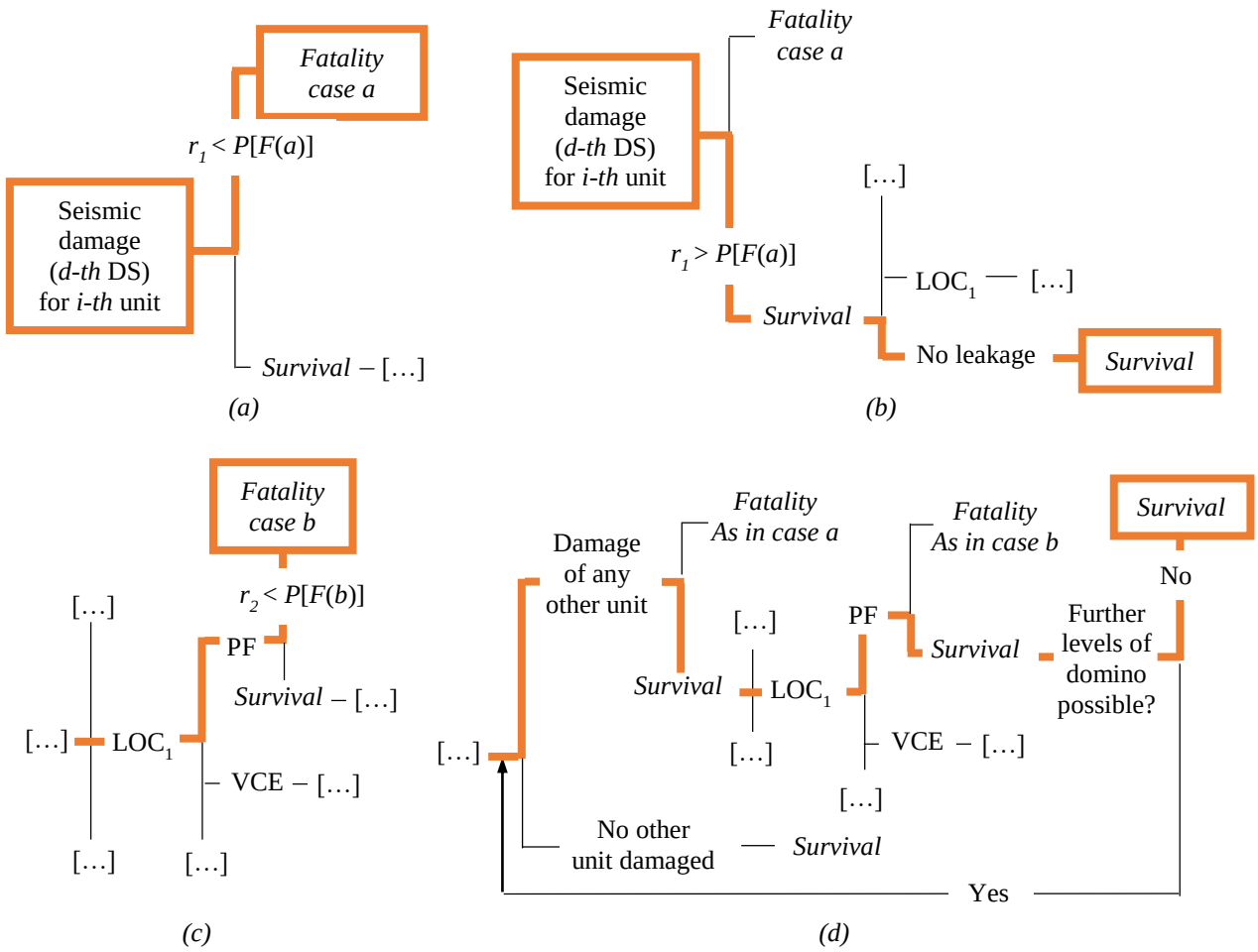

Figure 6. Different examples of Monte Carlo simulations: (a) "Fatality case a", (b) "Survival" outcome, (c) "Fatality case b", and (d) "Survival" outcome after domino effects

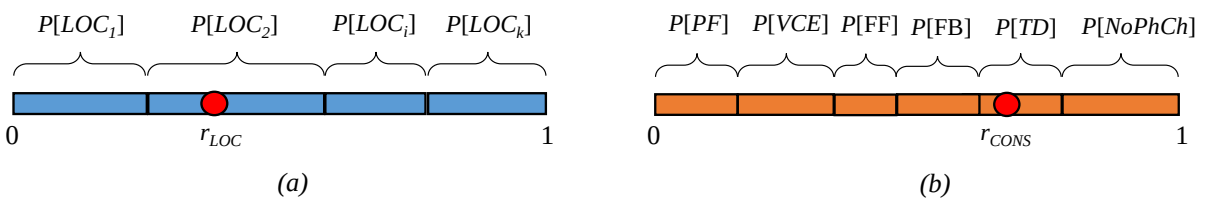

Figure 7. Schematic demonstration of sampling of: (a) LOC states, and (b) physical-chemical phenomena as a consequence of LOC states

A new random number r_2 between 0 and 1 is then generated and compared to the probability that the sampled physical-chemical phenomenon causes a fatality, $P[F(b)]$. If r_2 is less than $P[F(b)]$, then the outcome of the simulation is "*Fatality*", and the simulation is terminated (Figure 6c). Otherwise, if r_2 is greater than $P[F(b)]$, a domino effect must be further simulated. Therefore, the simulation continues as presented by the event tree in Figure 4. If the number of units in a system is n_U, it is necessary to generate (n_U -1) random numbers between 0 and 1, i.e. one random number for each of the other units in the system. If the value of the random number is less than the probability of damage due to physical-chemical phenomenon, $P[D(U)|PhCh]$, the unit is considered to be damaged. At this point, the simulation continues according to the event tree presented Figure 4 in the same way as described for the event tree in Figure 3. The simulation eventually stops when the outcome is "*Survival*" (e.g. Figure 6d) or "*Fatality*".

This paper was published in Relibility Engineering & System Safety. Please cite it as:
Celano F, Dolšek M. Fatality risk estimation for industrialized urban areas considering multi-hazard domino effects triggered by earthquakes, Relibility Engineering & System Safety, 2021, 206, 107287, https://doi.org/10.1016/j.ress.2020.107287.

The outcome for each MC simulation is "*Fatality*" or "*Survival*". Because the MC simulations are based on probability models as defined in Section 3, they are not computationally demanding, and it is relatively easy to perform a high number of simulations. Eventually, the probability $P[F(x,y)\,|\,D(U_i)=DS_d]$ is obtained as the ratio between the number of "*Fatality*" outcomes, N_F, divided by the total number of performed simulations, N_S:

$$P[F(x,y)\,|\,D(U_i)=DS_d]=\frac{N_F}{N_S} \tag{13}$$

The evaluation of Eq. (14) by implementing the MC method provides only the probability of fatality due to the *d-th* damage state for the *i-th* unit. The MC method must then be implemented $n_U \times n_{DS,i}$ times in order to calculate $n_U \times n_{DS,i}$ values of $P[F(x,y)\,|\,D(U_i)=DS_d]$, where each value corresponds to the probability of fatality at target (x,y) due to the *d-th* damage state for the *i-th* unit. Therefore, the probability $P[F(x,y)\,|\,IM=im]$ (Eq. (4)) can finally be computed.

2.4. Workflow for computation of fatality risk maps

The workflow of processes which result in IR and fatality risk maps is presented in Figure 8 in order to give an overall view of the computations. The computation of IR in an industrialized urban area begins with the discretization of the area in a grid of n_t targets. The n_U units in the area are then identified. In general, there may be many types of units in an industrial facility, such as tanks, vessels, or pipe racks, and other buildings outside the facility, such as offices and residential buildings. A discrete set of n_{DS} damage states must be defined for each of the identified units. In addition, the LOC states must be defined for the industrial units, which store hazardous material. The input data for the methodology are the models for the probability of events from the event trees, which are addressed in Section 3. Such models are needed to compute $P[F(x,y)\,|\,D(U_i)=DS_d]$ using the MC method (Subsection 2.3). In addition, required input data are the seismic fragility functions for all the damage states of all the units and the seismic hazard curve for the location of the industrialized urban area under investigation.

After the input data are prepared, the computation begins with the selection of the first target (x,y). The first unit and the first damage state are selected, and the probability of fatality at the selected target, $P[F(x,y)\,|\,D(U_i)=DS_d]$, is computed using the MC method (Subsection 2.3, Eq. (14)). The MC method is then implemented $n_U \times n_{DS}$ times in order to obtain the probability $P[F(x,y)\,|\,D(U_i)=DS_d]$ for all the n_U units and the corresponding $n_{DS,i}$ damage states. After the probabilities $P[D(U_i)=DS_d\,|\,IM=im]$ are obtained from the seismic fragility functions, the annual rate of fatality λ at the target can be calculated by Eq. (11). Finally, the IR at the target is estimated by Eq. (13). Then, another target is selected, and the procedure is repeated for all the targets in the grid (see the loop in Figure 6). The values for IR, which are eventually estimated for all targets in the grid, represent the basis for the evaluation of fatality risk maps, which are obtained by plotting iso-risk curves, i.e. curves characterized by the same values of IR, for the investigated area of interest.

This paper was published in Relibility Engineering & System Safety. Please cite it as:
Celano F, Dolšek M. Fatality risk estimation for industrialized urban areas considering multi-hazard domino effects triggered by earthquakes, Relibility Engineering & System Safety, 2021, 206, 107287, https://doi.org/10.1016/j.ress.2020.107287.

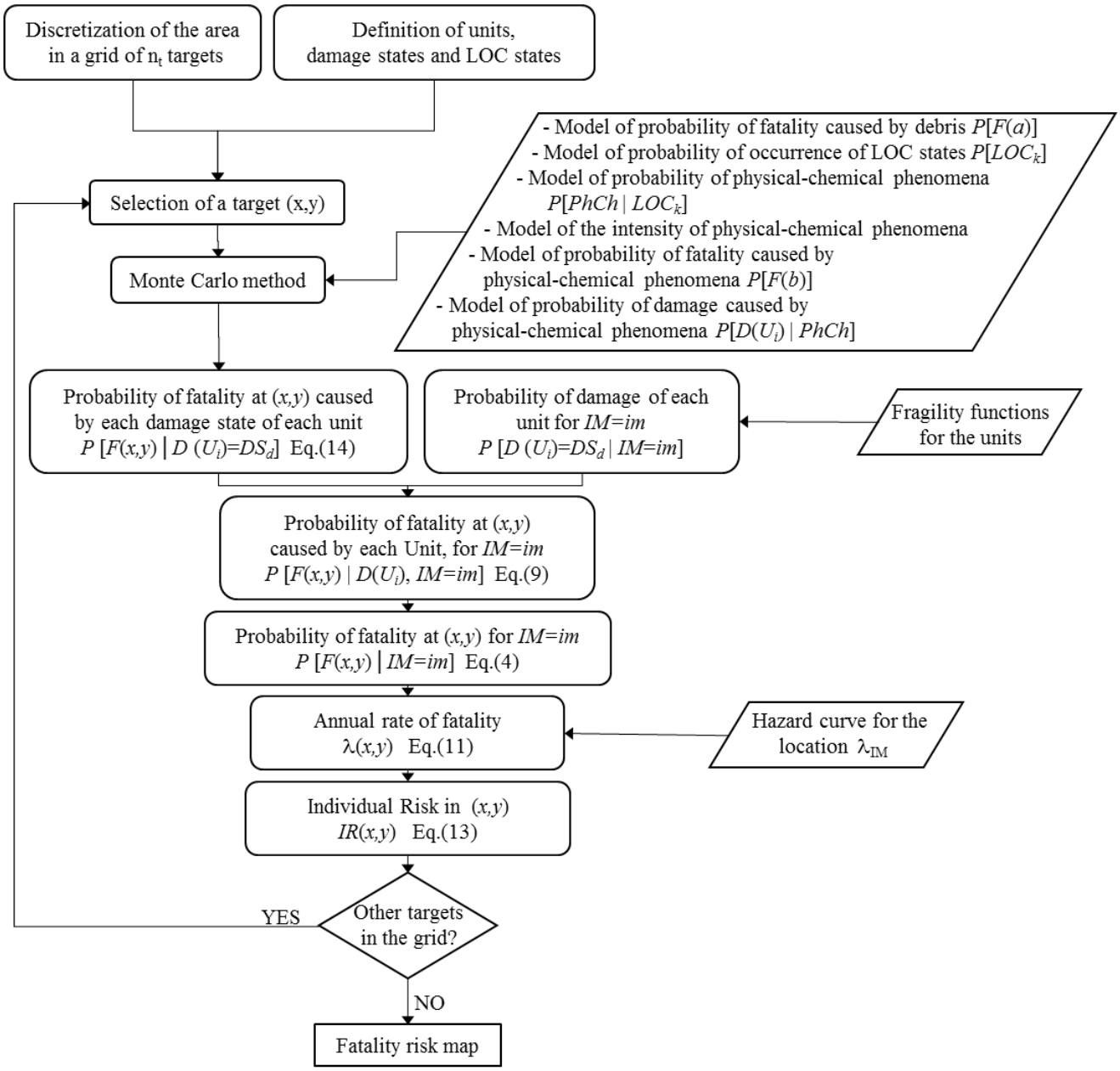

Figure 8. Workflow for the computation of individual risk and fatality risk map

3. Models of probabilities for the intermediate events in the event trees

In this section, the models of probabilities for the events in the event trees (Figure 3 and Figure 4) are described. These models are needed for the application of the MC method, but they are not based on empirical probabilities of fatality caused by historical earthquakes, which would naturally account for domino effects. Such empirical data would not be sufficient, because domino effects can evolve in many different ways, and the empirical data from past events may not cover all the possible scenarios. Moreover, major earthquakes are rare. Thus their catastrophic effects were not often observed in the industrialized urban areas. The approach presented in this paper, instead, is based on models of the probability of fatality that are specific for different hazards (e.g. fatality due to structural damage, fires, explosions, toxic dispersion, etc.), as presented in the following. These models may be improved and validated by empirical data of fatalities collected for the distinct

hazards, which do not naturally account for domino effects. Such data are more frequent, whereas it is difficult to expect that empirical fatality models will be soon available.

3.1 Probability of fatality as a direct consequence of seismic damage to the unit (*fatality case a*)

The estimation of the probability of fatality as a direct consequence of seismic damage to the unit, $P[F(a)]$, is quite a complex problem. In general, the $P[F(a)]$ depends on the type of unit and the severity of the damage state. Moreover, the distance between the *i-th* unit and the target significantly affects $P[F(a)]$, i.e. an individual will not be injured by debris falling from a unit if the unit is far from him. Therefore, it will be assumed that *fatality case a* can only happen if the target (x,y) and the source unit occupy the same position on the grid.

One option for the estimation of $P[F(a)]$ is to use empirical historical data. For example, NOAA [25] published a work in which the fatalities due to major earthquakes in the USA between 1860 and 1971 were estimated. Later, the Applied Technology Council [26] provided estimates for fatalities based on building types and damage states. Zuccaro and Cacace [27] also provided fatality probabilities for different damage states of residential buildings. The authors considered six damage states (D0, no damage; D1, slight damage; D2, moderate damage; D3, heavy damage; D4, very heavy damage; and D5, collapse), and defined nonzero fatality probabilities only for the D4 and D5 damage states. Furthermore, the Federal Emergency Management Agency [28] provided fatality ratios for several kinds of building typologies and four different damage states. Nevertheless, there is still a significant lack of data on collapse-related fatality ratios for industrial units. However, data from [28] showed that these fatality ratios do not change significantly for different structure typologies. For this reason, the same probabilities $P[F(a)]$ were assumed for all the typologies of units in the system.

3.2 Probability of occurrence of LOC states

The model used for estimating the probabilities of LOC states, $P[LOC_k]$, must simulate the occurrence of an LOC state in the case that a unit is part of an industrial facility which contains hazardous material. In this study, the LOC states defined in the Purple Book [17] and also used in [29] were considered:

- LOC_1: *minor loss*, defined as the continuous release of partial or total inventory over a time interval of more than 10 min,
- LOC_2: *intense loss*, defined as the continuous loss of total inventory within 10 min,
- LOC_3: *catastrophic loss*, defined as the instantaneous loss of inventory.

The probability of occurrence of each LOC state, in general, depends on the severity of the *d-th* damage state. Indeed, it is evident that the probability of having a catastrophic LOC is greater in the case of a more severe damage state. However, although the relationship between damage state and LOC state should be described by probabilistic models, it is more common in the literature for authors to use deterministic models [10,29]. This means that the probability of occurrence of the *k-th* LOC state conditioned to the occurrence of the *d-th* damage state is assumed to be 0 or 1. However, more precise models for $P[LOC_k]$ can also be used with the proposed probabilistic framework for the calculation of IR.

3.3 Probability of occurrence of physical-chemical phenomena as a consequence of LOC states

After the occurrence of an LOC state, different physical-chemical phenomena (PF, VCE, etc.) may be triggered, as discussed in the previous section. In the general case, these phenomena depend on the severity of the LOC state and on the type of released material, which may be flammable or toxic. After the type of released

This paper was published in Relibility Engineering & System Safety. Please cite it as:
Celano F, Dolšek M. Fatality risk estimation for industrialized urban areas considering multi-hazard domino effects triggered by earthquakes, Relibility Engineering & System Safety, 2021, 206, 107287, https://doi.org/10.1016/j.ress.2020.107287.

hazardous material is known, the probabilities of physical-chemical phenomena conditioned to the occurrence of the *k-th* LOC state must be estimated, $P[PhCh|LOC_k]$. In practice, this problem is usually treated in a simplified manner. For example, Vílchez et al. (2011) [24] presented a set of default values for the probabilities $P[PhCh|LOC_k]$ of the most common types of hazardous materials and LOC states. They considered that, after a LOC event, the incident could evolve in different ways, depending on the type of hazardous material involved. In particular, in the case of leakage of hazardous material, there might be an immediate ignition or a delayed ignition. Therefore, the probability of a physical-chemical phenomenon is related to the probabilities of immediate and delayed ignitions of the hazardous material. The probabilities of ignition in [24] are based on information found in the literature (e.g. [17]) and expert judgment.

The same approach, based on default probabilities, was also used in [7,10] and many others. Table 1 summarizes the probabilities of occurrence of the physical-chemical phenomena presented in Subsection 2.2, for some types of stored materials [24]. It should be noted that the event "No physical-chemical phenomena" is also considered ("*No PhCh*" in Table 1). If the *i-th* unit under consideration is an industrial unit which does not store hazardous material, then the probability of the event "No physical-chemical phenomena" is equal to 1. Otherwise, in the case of hazardous materials, the probabilities are derived from [24]. In many cases, the probabilities are the same for all three types of LOC events considered. The physical-chemical phenomena are considered to be mutually exclusive, which means that the sum of the probabilities along each line must always be equal to 1.

Table 1. Probability of occurrence of physical-chemical phenomena as a consequence of LOC states [24]

Type of material	LOC state	$P[TD]$	$P[PF]$	$P[FF]$	$P[VCE]$	$P[FB]$	$P[No\ PhCh]$
Not hazardous	LOC 1, 2, 3	0	0	0	0	0	1
Flammable liquids	LOC 1, 2, 3	0	0.01	0	0	0	0.99
Toxic, flammable liquids	LOC 1, 2, 3	0.99	0.01	0	0	0	0
Flammable, volatile liquids	LOC 1, 2, 3	0	0.065	0.561	0.374	0	0
Fully refrigerated flammable liquids	LOC 1, 2, 3	0	0.7	0.18	0.12	0	0
Toxic gases	LOC 1, 2, 3	1	0	0	0	0	0
Extremely flammable, pressurized liquefied gases	LOC 1, 2	0	0.7	0.18	0.12	0	0
	LOC 3	0	0.126	0.18	0.204	0.49	0
Toxic, extremely flammable, pressurized liquefied gases	LOC 1, 2	0.3	0.7	0	0	0	0
	LOC 3	0.3	0.126	0	0.084	0.49	0

3.4 Models for the intensity of physical-chemical phenomena

In order to evaluate the probability of fatality due to the physical-chemical phenomena, it is necessary to model the intensity of such phenomena at all the targets of the investigated area. The intensity of each physical-chemical phenomenon is mainly described by one or more physical-chemical intensity measures. For instance, in the case of pool fire and flash fire, the most important intensity measure describing the phenomenon is heat radiation. In the case of explosion and the case of toxic dispersion, the intensity measures are, respectively, the overpressure and the concentration of toxic material in the air. In the following, the models for evaluating the

intensity of physical-chemical phenomena are presented. They are then used in the following section as an input parameter for the evaluation of fatality probability due to *fatality case b*.

Heat radiation in the case of pool fire

A pool fire is the uncontrolled combustion of vapours generated by a pool of a flammable liquid. Because of the temperature difference between the hot gases of the flame and the objects in the environment, the heat released from the fire is transferred to the surroundings. This problem is considered in the Yellow Book [23], which is a manual entitled "Methods for the calculation of physical effects due to releases of hazardous materials (liquids and gases)" and elaborated by The Netherlands Organization of Applied Scientific Research (TNO). This manual provides an extensive overview of the models available in the literature to estimate the heat radiation produced by a pool fire. These models also allow for simulation of the radiating heat with respect to distance from the point source. In particular, it is assumed that the heat radiation is spread isotropically from a single point source, located at the centre of the pool fire. The pool fire is represented as a cylinder over the surface of the liquid fuel, characterized by diameter D_F and height H_F, which are correlated by the following equation:

$$\frac{H_F}{D_F} = 55\left(\frac{m''}{\rho_{air}\left(g \cdot D_F\right)^{1/2}}\right)^{0.67} \cdot \underline{u}^{-0.21} \tag{14}$$

where m'' is the burning mass rate per unit area and unit time (in kg/(m^{2}s)), ρ_{air} is the density of the air, g is the acceleration of gravity, and $\underline{u}$ is the scaled wind velocity at the height of 10 m (see [23] for details). The burning mass rate can be calculated as follows [23]:

$$m'' = m''_{\infty} \cdot \left(1 - e^{\tilde{k} \cdot \tilde{\beta} \cdot D_F}\right) \tag{15}$$

where m''_{∞} is the burning mass loss rate per unit time for an infinite pool diameter, and k and β are empirical constants. The Yellow Book [23] provides values of m''_{∞}, $\tilde{k}$, and $\tilde{\beta}$ for different hazardous materials. For example, $m''_{\infty} = 0.055$ and $\tilde{k} \cdot \tilde{\beta} = 2.10$ are given for gasoline.

In the model used by the Yellow Book [23], the heat radiation HR (in J/(m^{2}s)) decreases with the inverse square of the distance x between the point source and the target, as given by the following equation:

$$HR = \frac{(\pi \cdot D_F \cdot H_F + \pi \cdot D_F{}^2 / 4) \cdot F_s \cdot m'' \cdot \Delta H_c}{(c_1 \cdot m''^{0.61} + 1) \cdot 4\pi x^2} \tag{16}$$

where F_s is the fraction of combustion heat radiated from the flame surface, c_1 is a constant, and ΔH_c is the heat of combustion of flammable material at its boiling point (in J/kg).

The presented model thus allows for estimating the heat radiation generated by a pool fire with respect to the distance from the source. However, it is worth noting that the models presented herein for the evaluation of the effects of pool fires can be replaced by sophisticated models. An example may be found in [30].

Heat radiation in the case of flash fire

A flash fire can be triggered if the released combustible gas is not ignited immediately, but instead forms a vapour plume which is dispersed into the ambient air and later on ignited. Because the flash fire is characterized by a very short duration, it can be assumed that such a phenomenon is not likely to result in domino effects, as shown in [5]. However, the flame impingement resulting from the flash fire may cause the direct ignition of

This paper was published in Relibility Engineering & System Safety. Please cite it as:
Celano F, Dolšek M. Fatality risk estimation for industrialized urban areas considering multi-hazard domino effects triggered by earthquakes, Relibility Engineering & System Safety, 2021, 206, 107287, https://doi.org/10.1016/j.ress.2020.107287.

flammable material contained in an industrial unit, which generates a delayed pool fire [18]. For this reason, in the framework of this study, it is assumed that the flash fire results in a pool fire and the heat radiation is calculated as explained above.

Heat radiation in the case of fireball

In the case of the leakage of liquefied gases, the liquid can become a two-phase mixture, which forms a droplet cloud rich in fuel and typically results in a fireball. The physical parameter that is considered in the case of a fireball is the heat radiation, as in the case of pool fires. The heat radiation can be calculated as a function of the distance between the point source and the target in accordance with the Yellow Book [23]. Details are omitted in this paper for the sake of brevity.

Concentration of toxic material in the air

Toxic hazardous material released into the atmosphere can be dispersed by the wind. In the Yellow Book [23], several models that enable the prediction of this dispersion are provided. These models estimate the concentration of the released hazardous material at any location surrounding the point source of release. The most widespread model is the Gaussian Plume Model [31], which allows for estimating the concentration of the released material at a given place as a function of several variables, including the emission rate, the distance between the source and target, and the atmospheric conditions. The basic expression is the following [31]:

$$C(x,y,z)=\frac{q}{2\cdot\pi\cdot[\sigma_y(x)]\cdot[\sigma_z(x)]\cdot u}\cdot\exp\left(-\frac{y^2}{2\cdot[\sigma_y(x)]^2}-\frac{(h-z)^2}{2\cdot[\sigma_z(x)]^2}\right) \tag{17}$$

where x is the distance between the source and target in the wind speed direction (downwind distance), y is the distance perpendicular to the wind direction (crosswind distance), z is the height of the target point relative to the ground, q is the release rate, u is the wind velocity, σ_y, and σ_z are the so-called dispersion parameters, which are the function of the distance x, and h is the height of the release point relative to the ground. In the Yellow Book [23], formulations and tables are provided to calculate σ_y and σ_z as a function of the meteorological situation, which is described using Pasquill stability classes. Details are not given in this paper for the sake of brevity.

The release rate q is the quantity of material released within a unit of time. If there is a hole in the shell of a tank, this release rate depends on the size of the hole and can be estimated as in [23]:

$$q=A_h\sqrt{\gamma\rho_0P_0\left(\frac{2}{\gamma+1}\right)^{(\gamma+1)/(\gamma-1)}} \tag{18}$$

where A_h is the area of the hole, γ is the specific heat ratio of the gas, ρ_0 is the density of the gas in operating conditions, and P_0 is the pressure in operating conditions.

In this paper, the damage is described using a set of discrete damage states. Therefore, it is assumed that each damage state corresponds to an ideal area of the hole and that the hole is located at a height h relative to the ground (i.e. the height of release point). The presented model thus allows the estimation of the concentration of a released toxic gas with respect to the distance from the source. The concentration depends on the meteorological conditions, the properties of the released hazardous material, and the damage state of the industrial unit.

Overpressure and impulse due to vapour cloud explosion

This paper was published in Relibility Engineering & System Safety. Please cite it as:
Celano F, Dolšek M. Fatality risk estimation for industrialized urban areas considering multi-hazard domino effects triggered by earthquakes, Relibility Engineering & System Safety, 2021, 206, 107287, https://doi.org/10.1016/j.ress.2020.107287.

An explosion can be defined as the rapid release of energy into the atmosphere, which generates a blast wave. The physical parameters that describe a vapour cloud explosion are overpressure and impulse. The most widespread model used to estimate the overpressure and impulse as a function of the distance between source and target is the Multi-Energy model [23]. The Multi-Energy model provides blast charts (Figure 9), in which the scaled peak overpressure $\Delta P_s' = \Delta P_s / p_a$ and the scaled phase duration $t_p' = t_p / [(E_{\exp} / p_a)^{1/3} / c_0])$ are reported as a function of the scaled distance $x' = x / (E_{\exp} / p_a)^{1/3}$ for ten classes of blast strength (see [23] for details). ΔP_s is the overpressure caused by the explosion, p_a is the atmospheric pressure, t_p is the phase duration, $E_{\exp}$ is the explosion energy, c_o is the sound velocity, and x is the distance between the source of the explosion and the target.

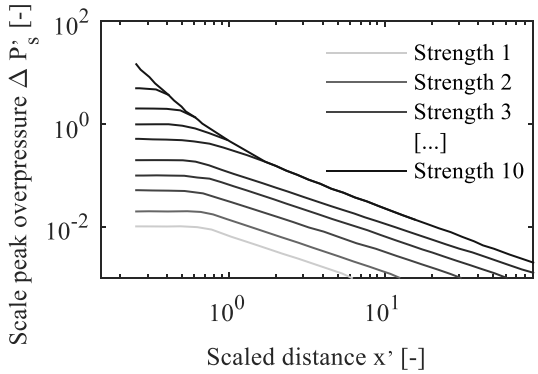

Figure 9. Blast chart from Multi Energy model [23]

The explosion energy E_{exp} is evaluated by multiplying the charge mass m_c with the specific heat of combustion ΔH_c [32]:

$$E_{\exp} = m_c \Delta H_c \tag{19}$$

The charge mass consists of the mass of the hazardous material (e.g. flammable gas) which is dispersed after the LOC. It is obtained by integrating the concentration $C(x,y,z)$ of the hazardous material over the entire volume of the hazardous material spread:

$$m_c = \int C(x,y,z)dxdydz \tag{20}$$

where the concentration $C(x,y,z)$ is estimated according to the model of concentration of toxic material (Eq. (18)). After the explosive energy is calculated, the blast chart (Figure 9) can be used to estimate the overpressure ΔP_s as a function of the distance between the source and target. The impulse I is then evaluated according to the Yellow Book [23]:

$$I = \frac{1}{2}\Delta P_s t_p \tag{21}$$

3.5 Probability of fatality caused by physical-chemical phenomena (*fatality case b*)

All the models from the previous subsection can be used to estimate the intensity of physical-chemical phenomena as a function of the distance between the source and target. This information is needed to compute the probability of fatality due to *fatality case b*, $P[F(b)]$ (see Subsection 2.2), which is a function of the intensity of the physical-chemical phenomena. It can thus be realized that $P[F(b)]$ depends on the type of

triggered physical-chemical phenomenon, the severity of the damage state of the unit, which affects the severity of the LOC state, and the distance between the source (i.e. the unit) and the target.

The most widespread models in literature for estimating the probability of fatality $P[F(b)]$ are based on "probit" functions [33], which are generally expressed as:

$$Y = a + b \cdot \ln(V) \tag{22}$$

where Y is the probit, V is a variable function of the intensity of the physical-chemical phenomenon, and a and b are so-called probit coefficients. In probability theory, the probit function is the quantile function associated with the standard normal distribution. Mathematically, it is the inverse of the Gaussian cumulative distribution function. Probit coefficients may be found in the Green Book [33], which is another manual elaborated by The Netherlands Organization of Applied Scientific Research (TNO), entitled "Methods for the determination of possible damage to people and objects resulting from the release of hazardous materials". Different probit coefficients are provided for cases of different intensity measures of physical-chemical phenomena. In the case of the concentration of toxic material, these coefficients may differ for different toxic materials. For example, Table 2 presents probit coefficients for the cases of radiation, overpressure, and the toxic release of ammonia (NH_3) [5]. In the same table, the method for calculating variable V for use in Eq. (23) is indicated. In particular, in the case of heat radiation, the V is the product $HR^{1.33}t_e$, where HR is the heat radiation in kW/m^2, estimated as explained in the previous sections for the case of pool fire, and t_e is the exposure time in seconds. In the case of overpressure, the V is the overpressure ΔP_s in psig (1 psig = 6.9 kPa), obtained as explained for the vapour cloud explosion. In the last case, where V is related to the intensity of toxic release, the V is the product C^2t_e, where C is the concentration of the toxic released material, expressed in ppm, and t_e is again the exposure time, expressed in minutes.

Table 2. Probit functions for estimating the probability of fatality due to chemical phenomena [5]

	a	b	V
Radiation	–14.9	2.56	$HR^{1.33}\,t_e$
Overpressure	1.47	1.37	ΔP_s
Toxic release of NH_3	–9.82	0.71	C^2t_e

Using the probit coefficients and the intensity of physical-chemical phenomena, which was provided by the models in the previous subsection as a function of source-target distances, the probit Y can be estimated according to Eq. (23). The general relationship between probit Y and probability $P[F(b)]$ is then expressed by the following equation [34]:

$$P\left[F(b)\right] = \frac{1}{\sigma\sqrt{2\pi}} \int_{-\infty}^{Y-5} \exp\left[-\left(\frac{V-\mu}{\sigma}\right)^2 \Big/ 2\right] dV \tag{24}$$

where μ and σ are median and variance of the Gaussian distribution, and V reflects the intensity of the physical-chemical phenomenon as defined in Eq.(23).

3.6 Probability of damage state of a unit caused by physical-chemical phenomena

A model for this probability is required because it is assumed that some of the physical-chemical phenomena may trigger a domino effect (see *fatality case c* in Subsection 2.2). The models available in the literature to estimate the probability of this event are again based on probit functions, and express the probit as a function of the intensity of the chemical-physical phenomena (Eq.(23)). The probit functions are different for the

This paper was published in Relibility Engineering & System Safety. Please cite it as:
Celano F, Dolšek M. Fatality risk estimation for industrialized urban areas considering multi-hazard domino effects triggered by earthquakes, Relibility Engineering & System Safety, 2021, 206, 107287, https://doi.org/10.1016/j.ress.2020.107287.

different types of units which may be damaged. In Table 3, the probit coefficients are summarized for different units and types of physical-chemical phenomena. They can be used to estimate the probability of collapse of residential buildings, storage warehouses, and tanks due to selected physical-chemical phenomena. It is assumed that residential buildings and storage warehouse can collapse only because of a vapour cloud explosion, and tanks can collapse because of vapour cloud explosions, pool fires and fireballs. The toxic dispersion alone does not cause structural damage. In addition, it has been shown before that flash fires are generally excluded from domino effect analysis because of the short duration of this phenomenon [18]. Because of the lack of data, the collapse of a unit will be the only damage state considered as possibly caused by the physical-chemical phenomenon.

Table 3. Probit functions for the estimation of the probability of collapse of a unit caused by physical-chemical phenomena. The parameters ΔP_s, I, HR, and Vol refer to peak overpressure in Pa, impulse in Pa·s, heat radiation in kW/m^2, and volume of target unit in m^3, respectively

	VCE			Reference
Target units	a	b	V	
Residential buildings Storage warehouses	5	–0.22	$\left(\frac{40000}{\Delta P_s}\right)^{7.4}+\left(\frac{460}{I}\right)^{11.3}$	The Green Book [33]
Tanks	–18.96	2.44	ΔP_s	Cozzani and Salzano (2004) [4]
	Pool fires and fireballs			
Target units	a	b	V	
Tanks	12.54	–1.85	$exp(-1.128\ ln(HR) - 2.2667 \cdot 10^{-5} Vol + 9.877)$	Cozzani et al. (2005) [5]

3.7 The uncertainties associated with the models of the probability of fatality

In the previous sections, the models used to evaluate the probability of fatality were presented. These models are coupled with the Monte Carlo method, as shown in Section 2.3. Particular attention was paid to the models for the intensity of physical-chemical phenomena, which are needed to estimate the intensity measures of pool fires, flash fires, toxic dispersions and vapour cloud explosions. As it was shown in Section 3.4, such computation requires the application of various mathematical models, assumptions, and empirically obtained data. However, the parameters associated with these model may include different kinds of variability, imprecision and uncertainty, as discussed in [35]. For example, it is difficult to choose the appropriate value of the wind velocity *u* because it is not possible to predict the exact meteorological condition when an accident occurs. Uncertainties also occur in the model of heat radiation in the case of pool fire, e.g. in calculating the pool shape, height, and extent [36]. The models of fatality due to the direct impact of the debris, the model of the probability of damage caused by chemical-physical phenomena and many others can also be considered uncertain.

In general, the uncertainties could be taken into account at least by considering that the parameters of the model are distributed according to given probability distributions. For example, for the case of Gaussian Plum Model, Siuta et al. (2013) [36] suggested using triangular distributions for wind velocity *u*. However, more sophisticated distributions can also be used if the relevant data are known. For example, Chutia (2017) [35] considered normal distributions for wind speed. These uncertainties and many others may be incorporated into MC simulations, through the random generation of the uncertain variables. In other words, at each simulation, all the uncertain parameters associated with models of the probability of fatality can be generated based on the adopted probability distribution functions, rather than assuming that their values are constant.

This paper was published in Relibility Engineering & System Safety. Please cite it as:
Celano F, Dolšek M. Fatality risk estimation for industrialized urban areas considering multi-hazard domino effects triggered by earthquakes, Relibility Engineering & System Safety, 2021, 206, 107287, https://doi.org/10.1016/j.ress.2020.107287.

The uncertainties discussed above are related to the models used to estimate the probability of fatality. However, there are many other sources of uncertainties. For example, seismic fragility functions considered for this methodology account for the record-to-record randomness but not for the effects of epistemic uncertainties. Consideration of such uncertainties may increase the risk of collapse of structures (e.g. [37]), which can affect the fatality risk too.

Because the proposed methodology is already quite complex, it was decided not to address the impact of uncertainty, although it may be substantial as discussed above. Therefore, the results presented in the following section are derived without considering the source of epistemic uncertainties, which is a topic for future research.

4. Application to a case study

The proposed methodology is demonstrated by developing fatality risk maps for a typical industrialized urban area, composed of industrial units and other units of the built environment. The IR is estimated for the entire area presented in Figure 10a. The layout of the investigated system, which is schematically presented in Figure 10b, consists of two tanks (TK1 and TK2), two storage warehouses (SW1 and SW2), and 33 residential buildings (RB1, RB2, etc.). In order to investigate the effects of earthquakes on such a system, it is assumed that the system is located in Priolo Gargallo, Sicily, which is a highly seismic event-prone area in the south of Italy where many industrial facilities can be found.

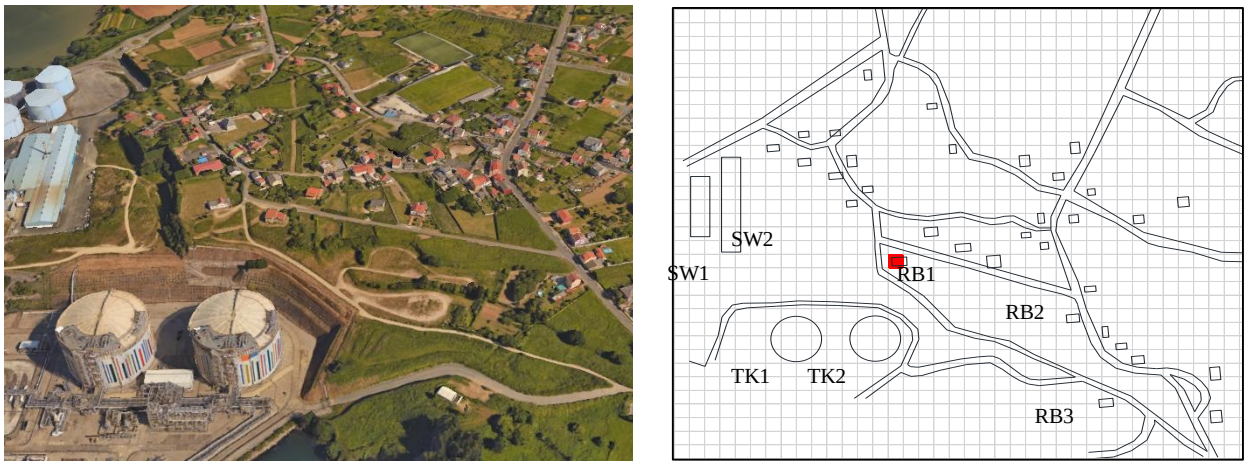

(a) *(b)*

Figure 10. (a) A typical industrialized urban area composed of industrial units and other units of the built environment [38], *and (b) layout of the investigated system with an indication of the units and the grid of targets. The red square identifies the target for which intermediate results are presented later in this section. For brevity, the notation is presented for only 3 residential buildings (RBs), while all 33 were considered in calculations*

The calculations were performed by following the processes in the flow chart (Figure 8). First, the area of interest was discretized into a grid of targets, defined by squares with dimensions of 25×25 m. Then, the units of the system were identified and defined. The two tanks are characterized by identical geometry, consisting of a diameter of 80 m and a height of 20 m. It was assumed that tank TK1 contained ammonia, which is a toxic gas, while tank TK2 contained gasoline, which is a flammable and volatile liquid. Note that the assumed configuration of the tanks does not reflect the industrialized area presented in Figure 10. It is also not likely that such configurations exist, but it was investigated in order to demonstrate the capability of the proposed methodology. The units of the system also include the storage warehouses, which were precast concrete buildings, and the residential buildings, which were considered to be reinforced concrete frame structures.

This paper was published in Relibility Engineering & System Safety. Please cite it as:
Celano F, Dolšek M. Fatality risk estimation for industrialized urban areas considering multi-hazard domino effects triggered by earthquakes, Relibility Engineering & System Safety, 2021, 206, 107287, https://doi.org/10.1016/j.ress.2020.107287.

The potential damage to each unit is classified with four (n_{DS} = 4) different damage states, which are described in Table 4. The damage states of the tanks are consistent with those defined in [39]. The damage states for the residential buildings were taken from [28]. The damage states for the storage warehouses were taken from [40]. The details are presented in Table 4. The LOC states for the tanks were defined in accordance with the Purple Book [17], and are thus classified as a *minor loss*, *intense loss*, and *catastrophic loss* LOC states.

Table 4. Definition and description of damage states of the units of the system

Damage state	Definition	Description of damage states		
		Residential building	Storage warehouse	Tank
DS1	Slight damage	Hairline cracks in some beams and columns	At least one non-structural component dislocated	Damage to roof other than buckling, minor loss of contents, minor damage to piping, no elephant's foot buckling
DS2	Moderate damage	Hairline cracks in most beams and columns	At least 50% of non-structural components dislocated	Elephant's foot buckling with minor loss of content
DS3	Extensive damage	Some of the frame elements have reached their ultimate capacity	All non-structural components dislocated	Elephant's foot buckling with major loss of content, severe damage, broken pipes
DS4	Collapse	Structural collapse	Structural collapse	Total failure, tank collapse

The relevant input data for the computation of the probability of fatality due to the damage state of a unit, $P[F(x,y)\,|\,D(U_i)=DS_d]$ are the models for the probability of intermediate events from the event trees. In the framework of this example, the following models were defined:

Probability of fatality caused by debris

In accordance to [27], it was assumed that the probability of fatality caused by debris, $P[F(a)]$, is equal to 0.08 for extensive damage (i.e. DS3), equal to 0.3 for the collapse damage state (i.e. DS4), and equal to 0 for DS1 and DS2. The same values of $P[F(a)]$ were taken into account for all the units of the system, even if these values were less reliable for the case of industrial units (such as tanks), which were not considered in the study of Zuccaro and Cacace [27].

Probability of occurrence of LOC states

The deterministic relationships between damage states and LOC states, as discussed in Subsection 3.2 and presented in Table 5, were considered. This is the simplest approach, but it is, however, also the most common in the literature (e.g. [10,29]).

Table 5. Probability of occurrence of LOC states for the four damage states considered

Damage state	$P[LOC_1]$	$P[LOC_2]$	$P[LOC_3]$
Slight damage	1	0	0
Moderate damage	0	1	0
Intense damage	0	1	0
Total collapse	0	0	1

Probability of occurrence of physical-chemical phenomena as a consequence of LOC states

The probabilities of occurrence of physical-chemical phenomena were derived from [24], as presented in Table 1 of Subsection 3.3. Because tank TK1 contains a toxic gas, the only possible physical-chemical phenomenon which could be triggered as a consequence of an LOC is a toxic dispersion, with probability $P[TD]$=1. In the

This paper was published in Relibility Engineering & System Safety. Please cite it as:
Celano F, Dolšek M. Fatality risk estimation for industrialized urban areas considering multi-hazard domino effects triggered by earthquakes, Relibility Engineering & System Safety, 2021, 206, 107287, https://doi.org/10.1016/j.ress.2020.107287.

case of tank TK2, which contains a flammable and volatile liquid, the possible physical-chemical phenomena which may be triggered are pool fires, with probability $P[PF]$=0.065, flash fires, with probability $P[FF]$=0.561, and vapour cloud explosions, with probability $P[VCE]$=0.374.

Models for the intensity of physical-chemical phenomena

Physical-chemical phenomena may be triggered both by an LOC from tank TK1 or from tank TK2. In the case of tank TK1, it is necessary to estimate the intensity of the concentration of the gas at the given distance between source and target, in order to simulate the effect of a toxic dispersion. Thus, the concentration of toxic gas was estimated using Eq.(18) as a function of the release rate q, which was calculated with Eq. (19). In order to calculate the release rate q, an equivalent area of the hole A_h in the industrial unit (i.e. the size of the damaged part) must be considered. For this purpose, the percentage of the total mass of material expected to be lost from the tank because of the damage state was obtained from [39]. In particular, it was expected that the percentage of lost content over a period equal to t_e would be 1%, 20%, 40%, and 100%, respectively, for DS1, DS2, DS3, and DS4. As a consequence, the area of the hole A_h, which increases with the severity of the damage state, was calculated to be consistent with a release equal to the percentage of content lost defined for each damage state over a period set to 15 min (as in [41]). For this calculation, only the Pasquill stability class F and the speed velocity u=2 m/s^2 were assumed, which is often considered to be the most conservative approach with respect to the extent of dispersion of toxic and flammable materials [18]. The resulting concentration of toxic gas is presented in Figure 11 as a function of the downwind and crosswind distances from the source of release, for the case of tank TK1 and damage state DS2. The σ_y, and σ_z were estimated as a function of the downwind distance and the Pasquill stability class F [23]. The considered toxic gas (i.e. ammonia) is characterized by the specific heat ratio γ=1.32 and by density ρ_0=0.73 kg/m^3. It was assumed that the pressure in operating conditions is the atmospheric pressure. Because the target is defined by an individual, the height z is assumed to be equal to 1.7 m. In order to make a conservative estimation, it was assumed that the wind was always blowing in the direction from the source to the target.

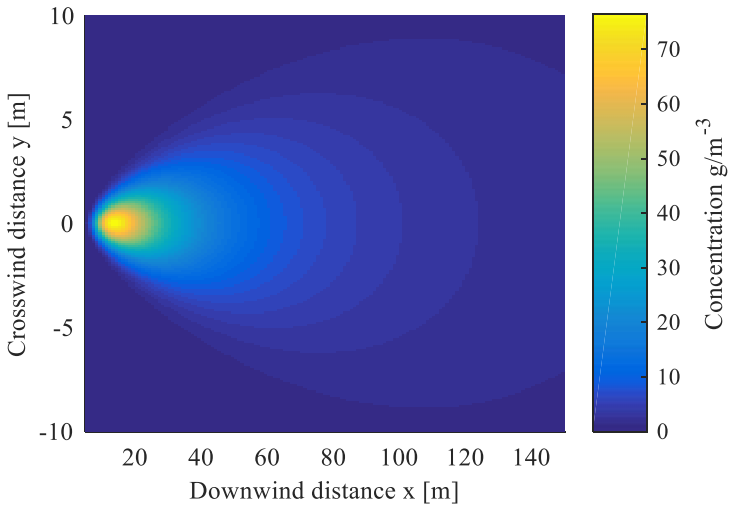

Figure 11. The concentration of toxic gas as a function of crosswind and downwind distances from the point source

Heat radiation as a function of the distance from the point source to the target must be modelled in the case of tank TK2. For this purpose, Eq. (17) was used, and the resulting heat radiation is presented in Figure 12a. The chemical characteristics of the gasoline in tank TK2 were $\Delta H_c = 44.0 MJ/Kg$, $F_s = 0.30$, $m''_\infty = 0.055$ and $\tilde{k} \cdot \tilde{\beta} = 2.10$ (from [23]). In the calculation, it was assumed that the diameter of the pool fire was equal to the diameter of the tank and that the wind coefficient was equal to 1. The blast charts from the Multi Energy model [23] (Figure 9) were used to estimate the expected impulse and overpressure as a function of the distance from the point source to the target, shown in Figure 12b, for the case of an LOC from tank TK2.

This paper was published in Relibility Engineering & System Safety. Please cite it as:
Celano F, Dolšek M. Fatality risk estimation for industrialized urban areas considering multi-hazard domino effects triggered by earthquakes, Relibility Engineering & System Safety, 2021, 206, 107287, https://doi.org/10.1016/j.ress.2020.107287.

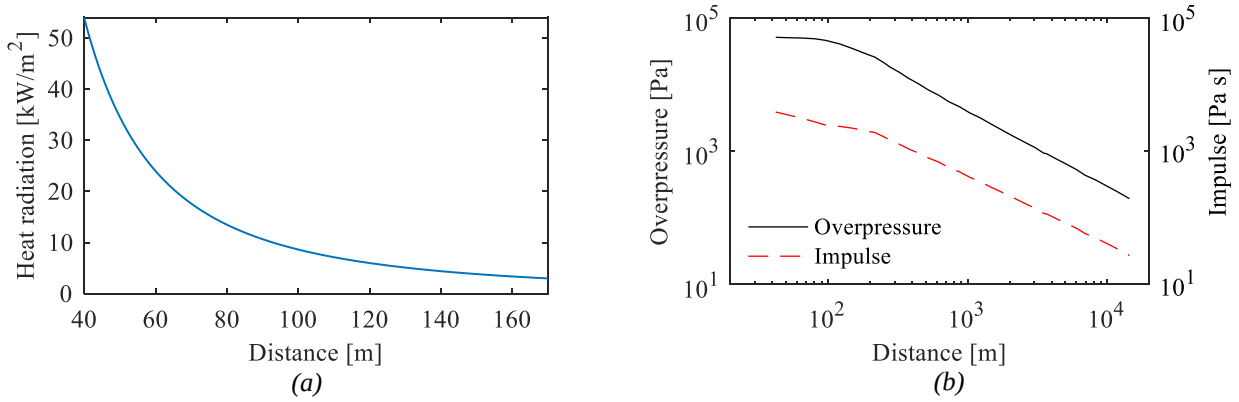

Figure 12. (a) Pool fire heat radiation as a function of the distance from the point source to the target [33] *for the case of tank TK2, containing gasoline, and (b) impulse and overpressure following a Vapour Cloud Explosion as a function of the source-target distance for the case of tank TK2, containing gasoline*

Probability of fatality and probability of damage states caused by physical-chemical phenomena

The probit functions presented in Subsections 3.5 and 3.6 were used to estimate the probability of fatality and the probability of damage to a unit caused by physical-chemical phenomena. The time of exposure was set to 15 min, which is consistent with the assumption made in [41].

On the basis of the described input data, the computation of $P[F(x,y)\,|\,D(U_i)=DS_d]$ began with implementing the MC simulations (as defined in Subsection 2.3). For the calculation of the probability of fatality in a particular target and with consideration of all damage states of all the units, $n_u \times n_{DS,i}$ sets of MC simulations were performed. Each set consisted of $2 \cdot 10^5$ simulations. The algorithm for MC simulations was developed in Matlab [42].

The probabilities of damage states $P[D(U_i)=DS_d\,|\,IM=im]$ have also to be estimated. For this purpose, it is necessary to consider the seismic fragility functions for each unit and each damage state. In this example, the parameters of the seismic fragility functions for the units were taken from the literature. The median seismic intensity causing a designated damage state, μ, and the corresponding logarithmic standard deviation, β, are presented in Table 6. The tanks were considered to be anchored, and seismic fragility functions were based on [28]. For the storage warehouse, the parameters of the seismic fragility functions were taken from [40] by assuming they belonged to Building class 9. The residential buildings were considered to be reinforced concrete buildings, and the corresponding seismic fragility functions were taken from [28]. All fragility functions were defined for peak ground acceleration (PGA). It should be noted that the seismic fragility functions used for this case study were not derived precisely for each unit of the industrialized urban area, but were adopted from the literature as presented in Table 6, for brevity of demonstration. However, the methodology is not limited to the definition of the damage states, and it can still be applied if seismic fragility functions are precisely derived for each unit of the system. For example, the fragility functions for storage tanks could be derived according to the procedure proposed by Phan et al. (2016) [43]. In such a case, the damage states would be associated with specific ranges of engineering demand parameters.

This paper was published in Relibility Engineering & System Safety. Please cite it as:
Celano F, Dolšek M. Fatality risk estimation for industrialized urban areas considering multi-hazard domino effects triggered by earthquakes, Relibility Engineering & System Safety, 2021, 206, 107287, https://doi.org/10.1016/j.ress.2020.107287.

Table 6. Parameters of seismic fragility functions for the system's units

Damage state	TK1, TK2		SWs		RBs	
	μ (g)	β	μ (g)	β	μ (g)	β
DS1	0.71	0.80	0.13	0.46	0.11	0.64
DS2	2.36	0.80	0.29	0.48	0.22	0.64
DS3	3.72	0.80	0.49	0.43	0.62	0.64
DS4	4.26	0.80	0.57	0.43	1.35	0.64

The probabilities of fatality due to damage of each unit, i.e. $P[(F(x,y)\,|\,D(U_i), IM = im)]$, were calculated according to Eq. (9). The Eq.(4) was then applied to calculate the probability of fatality at the target, $P[(F(x,y), IM = im)]$, for a range of PGA values between 0 and 4 g. The resulting probabilities are presented as a function of the PGA in Figure 13a, for the target indicated in Figure 10b (i.e. in the same position as the residential building RB1). The so-obtained curve was integrated together with the derivative of the seismic hazard function (Eq. (11)) in order to obtain the annual rate of fatality λ in the target (x,y). The seismic hazard function for Priolo Gargallo, shown in Figure 13b, was obtained using the software Reassess [44].

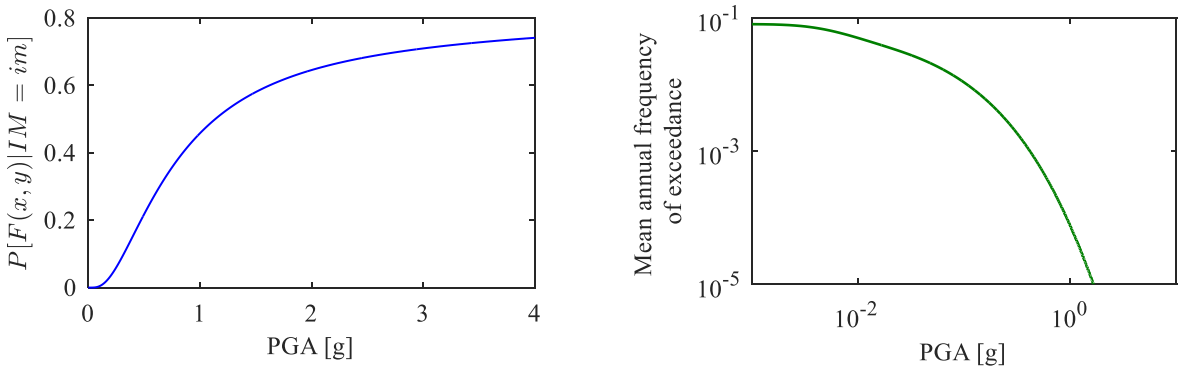

(a) *(b)*

Figure 13. (a) Probability of fatality at target (x,y) as a function of the intensity measure PGA; (b) hazard curve for Priolo Gargallo

The above-described procedure was repeated for all the targets in the grid (Figure 10b) in order to obtain the fatality risk over the entire area of interest. The computational time for the whole procedure was about 160 minutes. The methodology is not computationally very demanding because the simulation of the seismic response of the units is indirectly accounted through predefined seismic fragility functions (Table 6). However, if seismic fragility functions for the units are not available, they can be estimated by response history analysis before performing MC simulations. Running response history analysis of the system for each MC simulation would be computationally too demanding. In such a case, efficient structural reliability approaches may be used (e.g. [45,46]).

The resulting fatality risk map is shown in Figure 14. Different colours in the graph identify iso-risk curves, i.e. curves characterized by the same value of IR. It can be observed that the highest IR (most intense shade of red in Figure 14) is in the immediate surroundings of TK1, which contains ammonia. This is because the probability of a toxic dispersion in the case of the damage to a unit containing toxic gas is equal to 1 (Table 1), and the probability of fatality in the case of such a concentration of ammonia is very high. The fatality risk then decreases with distance from the tank, because the concentration in the atmosphere of the toxic gas also decreases. For greater distances from the tanks, the iso-risk curves become circular around TK2. This happens because the probability of fatality caused by leakage from the tank TK2 does not quickly decrease with the distance. The peaks for IR can also be observed in the immediate surroundings of the units because of the direct impact of debris (*fatality case a*).

This paper was published in Relibility Engineering & System Safety. Please cite it as:
Celano F, Dolšek M. Fatality risk estimation for industrialized urban areas considering multi-hazard domino effects triggered by earthquakes, Relibility Engineering & System Safety, 2021, 206, 107287, https://doi.org/10.1016/j.ress.2020.107287.

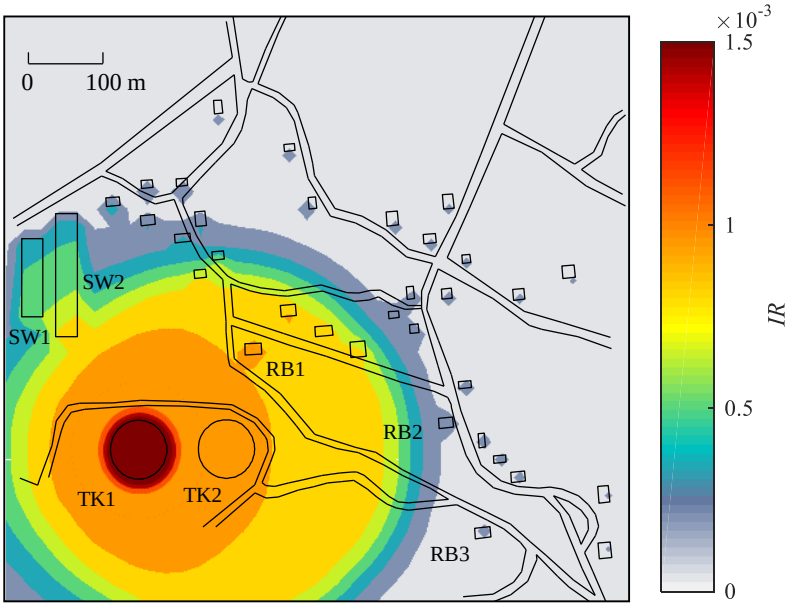

Figure 14. Fatality risk map of the individual risk (IR) for the presented case study by considering domino effects

It should be emphasized that Figure 14 presents the fatality risk map obtained by considering the domino effect. However, for the sake of comparison, the fatality risk map was also calculated by neglecting the domino effect (Figure 15). In this case, it was considered that a person standing at a target might die only because of the direct impact of debris, or because of the chemical consequences due to the leakage of hazardous material, i.e. *fatality case a* and *fatality case b*, as described in Subsection 2.2. It can be observed that the values of IR in the whole area are lower than those observed in the case when domino effects were considered. The circular iso-risk curves around tank TK2 occur due to high probability of fatality as a direct consequence of the leakage of hazardous material (*fatality case b*). The highest values of IR are observed again in the immediate surroundings of tank TK1. However, it should be noted that, in the case of Figure 14, tank TK1 can suffer damage because of the seismic event as well as because of the domino effect triggered by tank TK2. Namely, tank TK2 contains a flammable liquid, and that may cause a pool fire or a vapour cloud explosion. In the case of pool fire or the explosion of tank TK2, there is a high probability that tank TK1 will suffer structural damage and triggers toxic dispersion. However, this event is not considered in the results presented in Figure 15 because domino effects are disregarded. Therefore, not considering the domino effects in industrialized urban areas may lead to significant underestimation of the fatality risk in the case of a seismic event.

This paper was published in Relibility Engineering & System Safety. Please cite it as:
Celano F, Dolšek M. Fatality risk estimation for industrialized urban areas considering multi-hazard domino effects triggered by earthquakes, Relibility Engineering & System Safety, 2021, 206, 107287, https://doi.org/10.1016/j.ress.2020.107287.

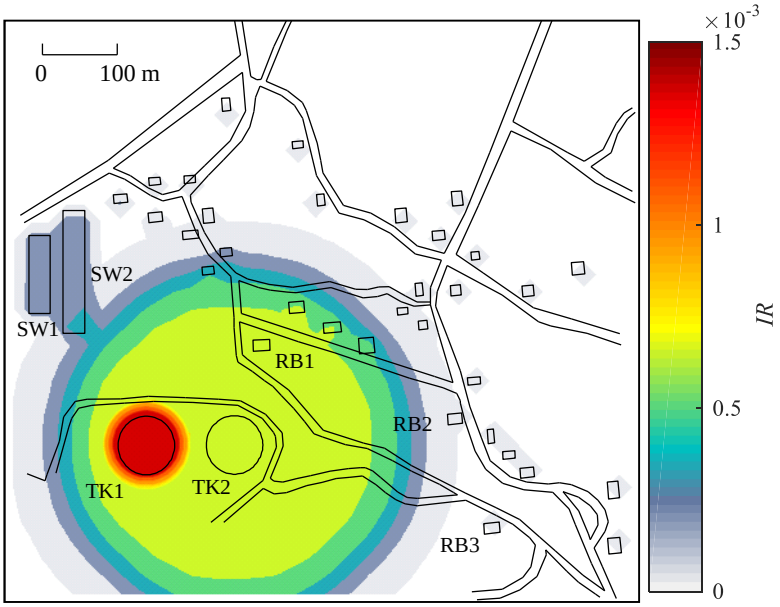

Figure 15. Fatality risk map of the individual risk (IR) for the presented case study without consideration of domino effects

It should be underlined that the fatality maps presented in Figure 14 and Figure 15 are obtained under the assumption of independent fatality events (see Eq. (7)), which provide the upper bound fatality risk. In order to investigate the overestimation of the fatality risk due to this assumption, the lower bound fatality risk and the corresponding fatality maps were derived by considering dependency between fatality events. Because the two tanks TK1 and TK2 store different types of hazardous materials, the full dependency between fatality events cannot be assumed. However, full dependency was assumed between the damage states of the two units. Tanks TK1 and TK2 are considered identical as far as the seismic response is regarded since they are characterized by the same fragility functions. Thus, the assumption of full dependency is limited to the structural damage of the two tanks TK1 and TK2. The fatality maps obtained under the assumption of full dependency between structural damage of the two tanks are presented in Figure 16 for the case with consideration and the case without consideration of domino effects.

By comparing fatality risk from Figure 16a and that from Figure 14, as well as by comparing Figure 16b and Figure 15, it can be concluded that the difference in the IR is observed only in the close surrounding of the tank TK1. In the remaining area, the fatality risk maps obtained under the assumptions of full independency and full dependency between structural damage of the two tanks, are only slightly different or practically the same. Therefore, the overestimation due to the assumption of full independency is limited to a small area surrounding TK1. However, this result is specific for the presented case study.

This paper was published in Relibility Engineering & System Safety. Please cite it as:
Celano F, Dolšek M. Fatality risk estimation for industrialized urban areas considering multi-hazard domino effects triggered by earthquakes, Relibility Engineering & System Safety, 2021, 206, 107287, https://doi.org/10.1016/j.ress.2020.107287.

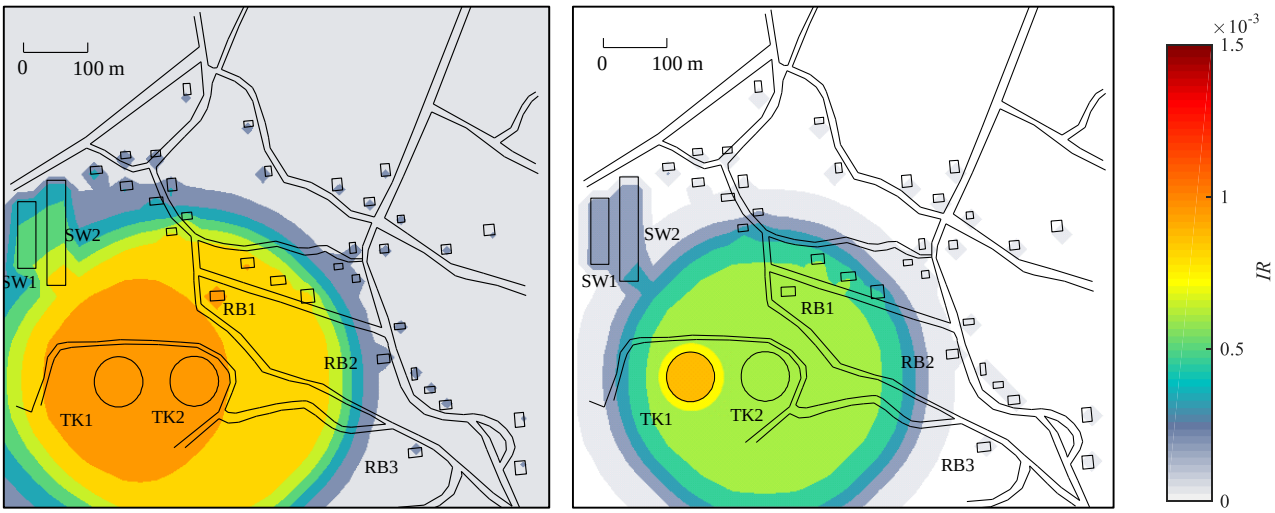

(a) *(b)*

Figure 16. The fatality risk map obtained by assuming full dependency between structural damage of the two tanks for the case (a) with and (b) without consideration of domino effects

The fatality risk maps can be used for decision-making regarding safety issues in industrialized urban areas. For this purpose, risk acceptance criteria may be found in the literature [47,48]. For instance, according to [47], the maximum tolerable IR in the case of nuclear facilities and onshore processes is equal to 10^{-4} per year. If this value of IR is considered as a threshold for the example presented in this study, then the iso-risk curve corresponding to an IR equal to 10^{-4} per year, as shown in Figure 17, defines the area which can be considered safe. Based on this information, stakeholders can rationally decide on actions to reduce risk in unsafe areas. Therefore, it is essential that risk studies account for all phenomena which may cause fatality events. For example, if multi-hazard domino effects were disregarded in this example, the iso-risk curve corresponding to an IR equal to 10^{-4} per year would be quite biased (Figure 17). This can be demonstrated by deriving the safety distances, i.e. the distances from a hazardous facility, along a given direction, at which the individual risk is less than the acceptable risk [49]. In particular, in Figure 17, the safety distances from the centre of the facility (point C in Figure 17), obtained with and without consideration of domino effects, are highlighted. When domino effects are neglected, the safety distance, along the direction presented in Figure 17, is equal to 360 m, while it is equal to 450 m when domino effects are taken into account. Therefore, for this specific case study, the consideration of domino effects increases safety distance for 23%. This again emphasizes the importance of considering domino effects in the risk assessment of industrialized urban areas. However, it should be underlined that the individual risk does not directly provide information on the expected number of fatalities, because it does not take into account, by definition, the actual population of the area. Further studies will, therefore, address the evaluation of the societal risk, which is the relationship between frequency and the number of people suffering from a specified level of harm from the realisation of specified hazards [15]. Contributions in this direction may be found in Tsang et al. (2018) [15] where a procedure to develop societal risk functions able to provide the expected number of fatalities due to a single hazard type or multiple hazards is proposed.

It should be noted that the results presented in this section are not related to any specific industrialized urban area. Moreover, it is worth to emphasize that the results are based on existing models of probability of fatality, which were taken from the literature, rather than on empirical fatality data collected from historical Natech events. Therefore, the presented example demonstrates the proposed methodology, while the results can be further improved by addressing the uncertainty and accuracy of the models of probability of fatality used in the presented cases study.

This paper was published in Relibility Engineering & System Safety. Please cite it as:
Celano F, Dolšek M. Fatality risk estimation for industrialized urban areas considering multi-hazard domino effects triggered by earthquakes, Relibility Engineering & System Safety, 2021, 206, 107287, https://doi.org/10.1016/j.ress.2020.107287.

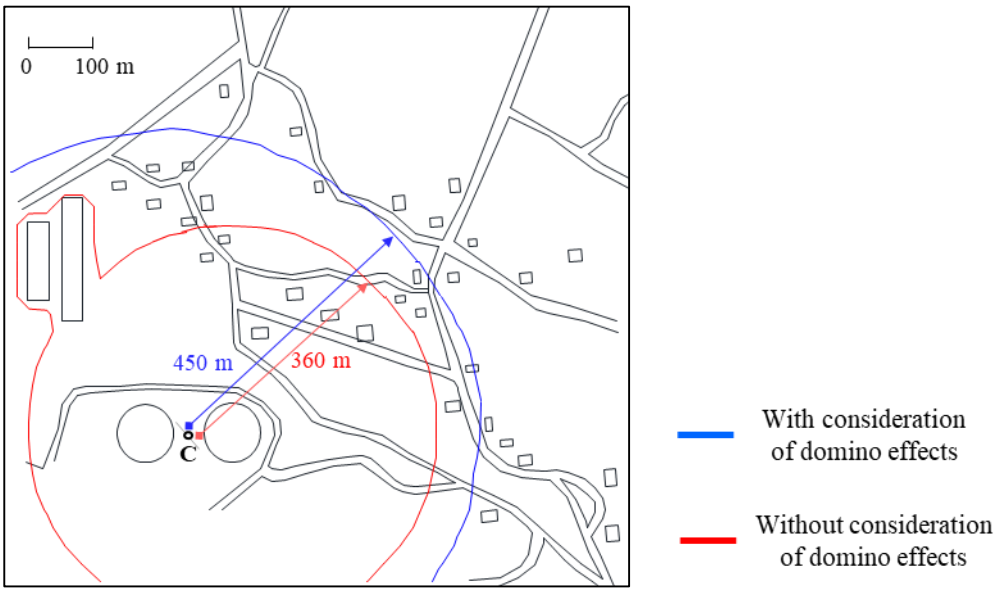

Figure 17. Iso-risk curves for IR=10^{-4} per year with and without consideration of domino effects

5. Conclusions

A methodology for earthquake fatality risk estimation in an industrialized urban area by considering domino effects was presented. It allows the simultaneous consideration of multiple hazards that endanger industrialized urban areas hit by an earthquake. The extremely complex phenomenon is decomposed into several subproblems. The seismic damage of the units is modelled by seismic fragility functions for different damage states, while earthquakes are modelled by the probabilistic seismic hazard analysis, as defined by seismologists. Several other models had to be defined, which, however, could generally be prepared by the involvement of different branches of engineering. These models are needed to simulate the probability of fatality caused by debris, the probability of loss of containment, the intensity of the triggered physical-chemical phenomena, and the probability of fatality and structural damage caused by such phenomena. All these models were integrated into the Monte Carlo method, which was used to calculate the individual risk and the fatality risk maps for the area of interest. Because these models simulate probabilities for different intermediate events, the computational efforts required for one simulation within the Monte Carlo method are minimized This allows to implement the method for complex problems which requires the simulation of multi-hazard domino effects. The methodology was primarily developed for areas influenced by petrochemical plants, but the theoretical part is general and can thus be applied to different types of industrialized urban areas.

The capabilities of the proposed methodology were demonstrated by calculating the fatality risk (i.e. individual risk, IR) maps with and without considering multi-hazard domino effects for a given industrialized urban area. It was shown that disregarding the domino effects in an industrialized urban area could lead to significant underestimation of risk in the case of seismic events. In particular, the distance from the hazardous facility at which the individual risk becomes less than the limiting value (IR=10^{-4} / year) was increased by 23% when domino effects were taken into account. Information from the fatality risk maps could be used for decision-making regarding safety issues in an industrialized urban area. However, the final goal of the research, which was a part of the XP-RESILIENCE project sponsored by the European Commission, was to develop the proposed methodology in order to use it for designing or upgrading units in an industrial facility.

Due to the extreme complexity of the problem, the proposed methodology is based on several simplifications and assumptions. Modelling of the relationship between damage states and loss of containment states is simplified. The effects of physical-chemical phenomena were obtained under several hypotheses (e.g. the effects of meteorological conditions were practically neglected). Also, the models which allow for estimating the probability of fatality and the probability of structural damage due to chemical phenomena are based on

probit functions, which are also quite simplified. Consequently, additional studies are needed to improve these models, which, however, can be treated by teams of engineers of different branches. Currently, the validation of the IR based on the proposed methodology is limited because of the limited availability of empirical fatality data collected from domino effects triggered by historical Natech events. However, the approach presented in this paper is based on independent models for the fatalities caused by different hazards (e.g. fatality due to structural damage or fires or explosions or toxic dispersion or other phenomena). The validation issue may thus be solved partly in future research, by validating the fatality models with empirical data obtained for different hazard, without considering the effect of domino. The potential bias in the estimation of the IR due to the lack of data is thus a subject of future research.

Acknowledgement

This research is part of the XP-RESILIENCE project, which is funded by the European Union's Horizon 2020 research and innovation programme under the Marie Sklodowska-Curie grant agreement No. 721816.

References

[1] Necci A, Cozzani V, Spadoni G, Khan F. Assessment of domino effect: State of the art and research needs. Reliab Eng Syst Saf 2015;143:3–18. doi:https://doi.org/10.1016/j.ress.2015.05.017.

[2] Kim H, Heo G, Jung S. QRA considering multi-vessel failure scenarios due to a natural disaster – Lessons from Fukushima. J Loss Prev Process Ind 2016;44:699–705. doi:https://doi.org/10.1016/j.jlp.2016.06.004.

[3] Reniers G, Cozzani V. Domino effects in the process industries. Elsevier; 2013. doi:https://doi.org/10.1016/B978-0-444-54323-3.02001-7.

[4] Salzano E, Cozzani V. The analysis of domino accidents triggered by vapor cloud explosions. Reliab Eng Syst Saf 2005;90:271–84. doi:https://doi.org/10.1016/j.ress.2004.11.012.

[5] Cozzani V, Antonioni G, Spadoni G. Quantitative assessment of domino scenarios by a GIS-based software tool. J Loss Prev Process Ind 2006;19:463–77. doi:https://doi.org/10.1016/j.jlp.2005.11.007.

[6] Cimellaro GP, Villa O, Bruneau M. Resilience-based design of natural gas distribution networks. J Infrastruct Syst 2014;21:5014005. doi:https://doi.org/10.1061/(ASCE)IS.1943-555X.0000204.

[7] Ahumada CB, Quddus N, Mannan MS. A method for facility layout optimisation including stochastic risk assessment. Process Saf Environ Prot 2018;117:616–28. doi:https://doi.org/10.1016/j.psep.2018.06.004.

[8] Abdolhamidzadeh B, Abbasi T, Rashtchian D, Abbasi SA. A new method for assessing domino effect in chemical process industry. J Hazard Mater 2010;182:416–26. doi:https://doi.org/10.1016/j.jhazmat.2010.06.049.

[9] Ramírez-Marengo C, Diaz-Ovalle C, Vázquez-Román R, Mannan MS. A stochastic approach for risk analysis in vapor cloud explosion. J Loss Prev Process Ind 2015;35:249–56. doi:https://doi.org/10.1016/j.jlp.2014.09.006.

[10] Alessandri S, Caputo AC, Corritore D, Giannini R, Paolacci F, Phan HN. Probabilistic risk analysis of process plants under seismic loading based on Monte Carlo simulations. J Loss Prev Process Ind 2018;53:136–48. doi:https://doi.org/10.1016/j.jlp.2017.12.013.

[11] Yang R, Khan F, Neto ET, Rusli R, Ji J. Could pool fire alone cause a domino effect? Reliab Eng Syst Saf 2020;202:106976. doi:https://doi.org/10.1016/j.ress.2020.106976.

[12] Hou L, Wu X, Wu Z, Wu S. Pattern identification and risk prediction of domino effect based on data

mining methods for accidents occurred in the tank farm. Reliab Eng Syst Saf 2020;193:106646. doi:https://doi.org/10.1016/j.ress.2019.106646.

[13] Tsang H, Wenzel F. Setting structural safety requirement for controlling earthquake mortality risk. Saf Sci 2016;86:174–83. doi:https://doi.org/10.1016/j.ssci.2016.02.028.

[14] Lazar Sinković N, Dolšek M. Fatality risk and its application to the seismic performance assessment of a building. Eng Struct 2020;205:110108. doi:https://doi.org/10.1016/j.engstruct.2019.110108.

[15] Tsang H, Daniell JE, Wenzel F, Werner AC. A semi-probabilistic procedure for developing societal risk function. Nat Hazards 2018;92:943–69. doi:10.1007/s11069-018-3233-z.

[16] Tsang H, Daniell JE, Wenzel F, Wilson JL. A universal approach for evaluating earthquake safety level based on societal fatality risk. Bull Earthq Eng 2020;18(1):273–96. doi:10.1007/s10518-019-00727-9.

[17] CPR18E. Guideline for quantitative risk assessment. The Hague, Netherlands: Committee for the Prevention of Disasters; 2005.

[18] Iervolino I, Accardo D, Tirri AE, Pio G, Salzano E. Quantitative risk analysis for the Amerigo Vespucci (Florence, Italy) airport including domino effects. Saf Sci 2019;113:472–89. doi:https://doi.org/10.1016/j.ssci.2018.12.019.

[19] Cornell CA, Jalayer F, Hamburger RO, Foutch DA. Probabilistic basis for 2000 SAC federal emergency management agency steel moment frame guidelines. J Struct Eng 2002;128:526–33. doi:10.1061/(ASCE)0733-9445(2002)128:4(526).

[20] Vamvatsikos D, Cornell CA. Incremental dynamic analysis. Earthq Eng Struct Dyn 2002;31:491–514. doi:10.1002/eqe.141.

[21] Ji J, Elnashai AS, Kuchma DA. An analytical framework for seismic fragility analysis of RC high-rise buildings. Eng Struct 2007;29:3197–209. doi:https://doi.org/10.1016/j.engstruct.2007.08.026.

[22] Pang R, Xu B, Kong X, Zou D. Seismic fragility for high CFRDs based on deformation and damage index through incremental dynamic analysis. Soil Dyn Earthq Eng 2018;104:432–6. doi:https://doi.org/10.1016/j.soildyn.2017.11.017.

[23] CPR14E. Methods for the Calculation of Physical Effects – Due to Releases of Hazardous Materials (Liquids and Gases). The Hague, Netherlands: Committee for the Prevention of Disasters; 2005.

[24] Vílchez JA, Espejo V, Casal J. Generic event trees and probabilities for the release of different types of hazardous materials. J Loss Prev Process Ind 2011;24:281–7. doi:https://doi.org/10.1016/j.jlp.2011.01.005.

[25] NOAA. A Study of Earthquake Losses in the San Francisco Bay Area: Data and Analysis. A Report for the Office of Emergency Preparedness. Washington, D.C. 1972.

[26] ATC. Earthquake Damage Evaluation Data for California. Washington, D.C.: Applied technology council; 1985.

[27] Zuccaro G, Cacace F. Seismic casualty evaluation: The Italian model, an application to the L'Aquila 2009 event. In: Spence R, So E, Scawthorn C, editors. Hum. casualties earthquakes, Springer, Dordrecht; 2011, p. 171–84. doi:https://doi.org/10.1007/978-90-481-9455-1_12.

[28] FEMA. Multi-hazard loss estimation methodology earthquake model, HAZUS-MH MR3 Technical Manual Washington, DC: Federal Emergency 2003.

[29] Salzano E, Cozzani V. A fuzzy set analysis to estimate loss intensity following blast wave interaction with process equipment. J Loss Prev Process Ind 2006;19:343–52. doi:https://doi.org/10.1016/j.jlp.2005.08.002.

[30] Jujuly MM, Rahman A, Ahmed S, Khan F. LNG pool fire simulation for domino effect analysis. Reliab Eng Syst Saf 2015;143:19–29. doi:https://doi.org/10.1016/j.ress.2015.02.010.

[31] Abdel-Rahman AA. On the atmospheric dispersion and Gaussian plume model. Proc. 2nd Int. Conf. Waste Manag. Water Pollution, Air Pollution, Indoor Clim., Corfu, Greece: 2008.

[32] Chen C, Khakzad N, Reniers G. Dynamic vulnerability assessment of process plants with respect to vapor cloud explosions. Reliab Eng Syst Saf 2020;200:106934. doi:https://doi.org/10.1016/j.ress.2020.106934.

[33] CPR16E. Methods for the determination of the possible damage. The Hague, Netherlands: Committee for the Prevention of Disasters; 2005.

[34] Finney DJ. Probit Analysis. Cambridge: Cambridge University Press; 1971.

[35] Chutia R. Uncertainty quantification under hybrid structure of probability-fuzzy parameters in Gaussian plume model. Life Cycle Reliab Saf Eng 2017;6:277–84. doi:10.1007/s41872-017-0028-2.

[36] Siuta D, Markowski AS, Mannan MS. Uncertainty techniques in liquefied natural gas (LNG) dispersion calculations. J Loss Prev Process Ind 2013;26:418–26. doi:https://doi.org/10.1016/j.jlp.2012.07.020.

[37] Dolsek M. Incremental dynamic analysis with consideration of modeling uncertainties. Earthq Eng Struct Dyn 2009;38:805–25. doi:https://doi.org/10.1002/eqe.869.

[38] Google. Reganosa. Retrived from https://www.google.com/maps/@43.4594135,-8.2390204,765m/data=!3m1!1e3 n.d.

[39] ALA. Seismic fragility formulations for water systems. American Lifelines Alliance; 2001.

[40] Babič A, Dolšek M. Seismic fragility functions of industrial precast building classes. Eng Struct 2016;118:357–70. doi:https://doi.org/10.1016/j.engstruct.2016.03.069.

[41] Cozzani V, Gubinelli G, Salzano E. Escalation thresholds in the assessment of domino accidental events. J Hazard Mater 2006;129:1–21. doi:https://doi.org/10.1016/j.jhazmat.2005.08.012.

[42] MATLAB. R2016a. Natick, Massachusetts: The MathWorks Inc.; 2016.

[43] Phan HN, Paolacci F, Alessandri S. Fragility analysis methods for steel storage tanks in seismic prone areas. Proc. ASME 2016 Press. Vessel. Pip. Conf., Vancouver, Canada: 2016.

[44] Chioccarelli E, Cito P, Iervolino I, Giorgio M. REASSESS V2.0: software for single- and multi-site probabilistic seismic hazard analysis. Bull Earthq Eng 2019;17:1769–93. doi:10.1007/s10518-018-00531-x.

[45] Xu J, Dang C. A new bivariate dimension reduction method for efficient structural reliability analysis. Mech Syst Signal Process 2019;115:281–300. doi:https://doi.org/10.1016/j.ymssp.2018.05.046.

[46] Xu B, Pang R, Zhou Y. Verification of stochastic seismic analysis method and seismic performance evaluation based on multi-indices for high CFRDs. Eng Geol 2020;264:105412. doi:https://doi.org/10.1016/j.enggeo.2019.105412.

[47] HSE. Reducing risks, protecting people. HSE Books; 2001.

[48] Stewart MG, Netherton MD. A probabilistic risk-acceptance model for assessing blast and fragmentation safety hazards. Reliab Eng Syst Saf 2019;191:106492. doi:https://doi.org/10.1016/j.ress.2019.05.004.

[49] Duijm NJ. Acceptance criteria in Denmark and the EU. The Danish Environmental Protection Agency; 2009.

This paper was published in Relibility Engineering & System Safety. Please cite it as:
Celano F, Dolšek M. Fatality risk estimation for industrialized urban areas considering multi-hazard domino effects triggered by earthquakes, Relibility Engineering & System Safety, 2021, 206, 107287, https://doi.org/10.1016/j.ress.2020.107287.